

WETCHIMP-WSL: Intercomparison of wetland methane emissions models over West Siberia

T. J. Bohn¹, J. R. Melton², A. Ito³, T. Kleinen⁴, R. Spahni^{5,6}, B. D. Stocker^{5,7}, B. Zhang⁸, X. Zhu^{9,10,11}, R. Schroeder^{12,13}, M. V. Glagolev^{14,15,16,17}, S. Maksyutov^{3,16}, V. Brovkin⁴, G. Chen¹⁸, S. N. Denisov¹⁹, A. V. Eliseev^{19,20}, A. Gallego-Sala²¹, K. C. McDonald¹², M. A. Rawlins²², W. J. Riley¹¹, Z. M. Subin¹¹, H. Tian⁸, Q. Zhuang⁹, and J. O. Kaplan²³

[1]{School of Earth and Space Exploration, Arizona State University, Tempe, AZ, USA}

[2]{Canadian Centre for Climate Modelling and Analysis, Environment Canada, Victoria, BC, Canada}

[3]{National Institute for Environmental Studies, Tsukuba, Japan}

[4]{Max Planck Institute for Meteorology, Hamburg, Germany}

[5]{Climate and Environmental Physics, Physics Institute, University of Bern, Bern, Switzerland}

[6]{Oeschger Centre for Climate Change Research, University of Bern, Bern, Switzerland}

[7]{Department of Life Sciences, Imperial College, Silwood Park Campus, Ascot, UK}

[8]{International Center for Climate and Global Change Research and School of Forestry and Wildlife Sciences, Auburn University, Auburn, AL, USA}

[9]{Department of Earth, Atmospheric, and Planetary Sciences, Purdue University, West Lafayette, IN, USA}

[10]{Natural Resource Ecology Laboratory, Colorado State University, Fort Collins, CO, USA}

[11]{Earth Sciences Division, Lawrence Berkeley National Laboratory, Berkeley, CA, USA}

[12]{City College of New York, City University of New York, New York, NY, USA}

[13]{Institute of Botany, University of Hohenheim, Stuttgart, Germany}

[14]{Moscow State University, Moscow, Russia}

- 1 [15]{Institute of Forest Science, Russian Academy of Sciences, Uspenskoe, Russia}
2 [16]{Laboratory of Computational Geophysics, Tomsk State University, Tomsk, Russia}
3 [17]{Yugra State University, Khanty-Mantsiysk, Russia}
4 [18]{Oak Ridge National Laboratory, Oak Ridge, TN, USA}
5 [19]{A. M. Obukhov Institute of Atmospheric Physics, Russian Academy of Sciences,
6 Moscow, Russia}
7 [20]{Kazan Federal University, Kazan, Russia}
8 [21]{Department of Geography, University of Exeter, Exeter, UK}
9 [22]{Department of Geosciences, University of Massachusetts, Amherst, MA, USA}
10 [23]{Institute of Earth Surface Dynamics, University of Lausanne, Lausanne, Switzerland}
11 Correspondence to: T. J. Bohn (theodore.bohn@asu.edu)

12

13 **Abstract**

14 Wetlands are the world's largest natural source of methane, a powerful greenhouse gas. The
15 strong sensitivity of methane emissions to environmental factors such as soil temperature and
16 moisture has led to concerns about potential positive feedbacks to climate change. This risk is
17 particularly relevant at high latitudes, which have experienced pronounced warming and
18 where thawing permafrost could potentially liberate large amounts of labile carbon over the
19 next 100 years. However, global models disagree as to the magnitude and spatial distribution
20 of emissions, due to uncertainties in wetland area and emissions per unit area and a scarcity of
21 in situ observations. Recent intensive field campaigns across the West Siberian Lowland
22 (WSL) make this an ideal region over which to assess the performance of large-scale process-
23 based wetland models in a high-latitude environment. Here we present the results of a follow-
24 up to the Wetland and Wetland CH₄ Intercomparison of Models Project (WETCHIMP),
25 focused on the West Siberian Lowland (WETCHIMP-WSL). We assessed 21 models and 5
26 inversions over this domain in terms of total CH₄ emissions, simulated wetland areas, and
27 CH₄ fluxes per unit wetland area and compared these results to an intensive in situ CH₄ flux
28 dataset, several wetland maps, and two satellite surface water products. We found that: a)
29 despite the large scatter of individual estimates, 12-year mean estimates of annual total

1 emissions over the WSL from forward models ($5.34 \pm 0.54 \text{ Tg CH}_4 \text{ y}^{-1}$), inversions (6.06
2 $\pm 1.22 \text{ Tg CH}_4 \text{ y}^{-1}$), and in situ observations ($3.91 \pm 1.29 \text{ Tg CH}_4 \text{ y}^{-1}$) largely agreed; b)
3 forward models using surface water products alone to estimate wetland areas suffered from
4 severe biases in CH_4 emissions; c) the interannual timeseries of models that lacked either soil
5 thermal physics appropriate to the high latitudes or realistic emissions from unsaturated
6 peatlands tended to be dominated by a single environmental driver (inundation or air
7 temperature), unlike those of inversions and more sophisticated forward models; d)
8 differences in biogeochemical schemes across models had relatively smaller influence over
9 performance; and e) multi-year or multi-decade observational records are crucial for
10 evaluating models' responses to long-term climate change.

11

12 **1 Introduction**

13 Methane (CH_4) emissions from high-latitude wetlands are an important component of the
14 global climate system. CH_4 is an important greenhouse gas, with approximately 34 times the
15 global warming potential of carbon dioxide (CO_2) over a century time horizon (IPCC, 2013).
16 Globally, wetlands are the largest natural source of CH_4 emissions to the atmosphere (IPCC,
17 2013). Because wetland CH_4 emissions are highly sensitive to soil temperature and moisture
18 conditions (Saarnio et al., 1997; Friberg et al., 2003; Christensen et al., 2003; Moore et al.,
19 2011; Glagolev et al., 2011; Sabrekov et al., 2014), there is concern that they will provide a
20 positive feedback to future climate warming (Gedney et al., 2004; Eliseev et al., 2008;
21 Ringeval et al., 2011). This risk is particularly important in the world's high latitudes, because
22 they contain nearly half of the world's wetlands (Lehner and Döll, 2004) and because the high
23 latitudes have been and are forecast to continue experiencing more rapid warming than
24 elsewhere (Serreze et al., 2000; IPCC, 2013). Adding to these concerns is the potential
25 liberation (and possible conversion to CH_4) of previously-frozen, labile soil carbon from
26 thawing permafrost over the next century (Christensen et al., 2004; Schuur et al., 2008; Koven
27 et al., 2011; Schaefer et al., 2011).

28 Process-based models are crucial for increasing our understanding of the response of wetland
29 CH_4 emissions to climate change. Large-scale biogeochemical models, especially those
30 embedded within earth system models, are particularly important for estimating the
31 magnitudes of feedbacks to climate change (e.g., Gedney et al., 2004; Eliseev et al., 2008;
32 Koven et al., 2011). However, as shown in the global Wetland and Wetland

1 CH₄ Intercomparison of Models Project (WETCHIMP; Melton et al., 2013; Wania et al.,
2 2013), there was wide disagreement among large-scale models as to the magnitude of global
3 and regional wetland CH₄ emissions, in terms of both wetland areas and CH₄ emissions per
4 unit wetland area. These discrepancies were due in part to the large variety of schemes used
5 for representing hydrological and biogeochemical processes, in part to uncertainties in model
6 parameterizations, and in part to the sparseness of in situ observations with which to evaluate
7 model performance (Melton et al., 2013).

8 In addition to these challenges at the global scale, the unique characteristics of high-latitude
9 environments pose further problems for biogeochemical models. For example, much of the
10 northern land surface is underlain by permafrost, which impedes drainage (Smith et al., 2005)
11 and stores ancient carbon (Koven et al., 2011) via temperature-dependent constraints on
12 carbon cycling (Schuur et al., 2008). Similarly, peat soils and winter snowpack can
13 thermally insulate soils (Zhang, 2005; Lawrence and Slater, 2008, 2010), dampening their
14 sensitivities to interannual variability in climate. Several commonly-used global
15 biogeochemical models (e.g., Tian et al., 2010; Hopcroft et al., 2011; Hodson et al., 2011;
16 Kleinen et al., 2012) lack representations of some or all of these processes.

17 The prevalence of peatlands in the high-latitudes poses further challenges to modeling
18 (Frolking et al., 2009). Peatlands are a type of wetland containing deep deposits of highly
19 porous, organic-rich soil, formed over thousands of years under waterlogged and anoxic
20 conditions, which inhibit decomposition (Gorham, 1991; Frolking et al., 2011). Within the
21 porous soil, the water table is often only a few centimeters below the surface, leading to
22 anoxic conditions and CH₄ emissions even when no surface water is present (Saarnio et al.,
23 1997; Friborg et al 2003; Glagolev et al 2011). This condition can lead to an underestimation
24 of wetland area when using satellite surface water products as inputs to wetland methane
25 emissions models. In addition, trees and shrubs are found with varying frequency in
26 peatlands (e.g., Shimoyama et al., 2003; Efremova et al., 2014), interfering with detection of
27 inundation. Furthermore, the water table depth within a peatland is typically heterogeneous,
28 varying on the scale of tens of centimeters as a function of microtopography (hummocks,
29 hollows, ridges, and pools; Eppinga et al., 2008). Models vary widely in their representations
30 of wetland soil moisture conditions, ranging from schemes that do not explicitly consider the
31 water table position (e.g., Hodson et al., 2011), to a single uniform water table depth for each
32 grid cell (e.g., Zhuang et al., 2004), to more sophisticated schemes that allow for sub-grid

1 heterogeneity in the water table (e.g., Bohn et al., 2007; Ringeval et al., 2010; Riley et al.,
2 2011; Kleinen et al., 2012; Bohn et al., 2013; Stocker et al., 2014; Subin et al., 2014). Finally,
3 peatland soils can be highly acidic and nutrient-poor, and much of the available carbon
4 substrate can be recalcitrant (Clymo et al., 1984; Dorrepaal et al., 2009). While some models
5 attempt to account for the effects of soil chemical conditions such as pH, redox potential, and
6 nutrient limitation (e.g., Zhuang et al., 2004; Riley et al., 2011; Sabrekov et al., 2013; Spahni
7 et al., 2013), not all do.

8 Given the potential problems of parameter uncertainty and equifinality (Tang and Zhuang,
9 2008; van Huissteden et al., 2009) and computational limitations when wetland components
10 are embedded within global climate models, it is important to determine which model features
11 are necessary to simulate high-latitude peatlands accurately, and to constrain parameter values
12 with observations. Until recently, evaluation of large-scale wetland CH₄ emissions models
13 has been difficult, due to the sparseness of in situ and atmospheric CH₄ observations.
14 However, observations from the West Siberian Lowland (WSL) now offer the opportunity to
15 assess model performance, thanks to recent intensive field campaigns (Glagolev et al., 2011),
16 aircraft profiles (Umezawa et al., 2012), tall tower observations (Sasakawa et al., 2010;
17 Winderlich et al., 2010), and high-resolution wetland inventories (Sheng et al., 2004; Peregon
18 et al., 2008; Peregon et al., 2009).

19 Our primary goal in this study is to determine how well current global large-scale models
20 capture the dynamics of high-latitude wetland CH₄ emissions. To this end, we assess the
21 performance of 21 large-scale wetland CH₄ emissions models over West Siberia, relative to in
22 situ and remotely-sensed observations as well as inverse models. We examine both spatial
23 and temporal accuracy, including seasonal and interannual variability, and estimate the
24 relative influences of environmental drivers on model behaviors. We identify the dominant
25 sources of error and the model features that may have caused them. Finally, we make
26 recommendations as to which model features are necessary for accurate simulations of high-
27 latitude wetland CH₄ emissions, and which types of observations would help improve future
28 efforts to constrain model behaviors.

29

1 **2 Methods**

2 **2.1 Spatial Domain**

3 The West Siberian Lowland (WSL) occupies approximately 2.5 million km² in North-Central
4 Eurasia, spanning from 50 to 75° N and 60 to 95° E (Figure 1a). This region is bounded on
5 the West by the Ural Mountains; on the East by the Yenisei River and the Central Siberian
6 Plateau; on the North by the Arctic Ocean; and on the South by the Altai Mountains and the
7 grasslands of the Eurasian Steppe (Sheng et al., 2004). The WSL contains most of the
8 drainage areas of the Ob' and Irtysh Rivers, as well as the western tributaries of the Yenisei
9 River, all of which drain into the Arctic Ocean. Permafrost in various forms (continuous,
10 discontinuous, isolated, and sporadic) covers more than half of the area of the WSL, from the
11 Arctic Ocean south to approximately 60° N, with continuous permafrost occurring north of
12 67° N (Kremenetski et al., 2003). The region's major biomes (Figure 1b) consist of the
13 treeless Tundra north of 66° N, approximately coincident with continuous permafrost; the
14 Taiga forest belt between 55 and 66° N; and the grasslands of the Steppe south of 55° N.

15 Wetlands occupy 600,000 km², or about 25% of the land area of the WSL, primarily in the
16 Taiga and Tundra zones (Sheng et al., 2004). The vast majority of these wetlands are
17 peatlands, with peat depths ranging from 50 cm to over 5 m, comprising a total soil carbon
18 pool of 70 Pg C (Sheng et al., 2004). Numerous field studies have documented strong
19 methane emissions from these peatlands, particularly those south of the southern limit of
20 permafrost (e.g., Sabrekov et al., 2014; Sasakawa et al., 2012; Glagolev et al., 2012; Glagolev
21 et al., 2011; Friberg et al., 2003; Shimoyama et al., 2003; Panikov and Dedysh, 2000).
22 Permanent water bodies, ranging in size from lakes 100 km² in area to pools only a few
23 meters across, are comingled with wetlands throughout the domain (Lehner and Döll, 2004;
24 Repo et al., 2007; Eppinga et al., 2008). Notable concentrations of lakes are found: a) north
25 of the Ob' River between 61 and 64° N and 68 and 80° E; b) west of the confluence of the
26 Ob' and Irtysh Rivers between 59 and 61° N and 64 and 70° E; and c) on the Yamal Peninsula
27 north of 68° N.

28 Because the vegetative and soil conditions vary substantially across the domain, we have
29 divided it into two halves of approximately equal size along 61° N latitude. The region north
30 of this line contains permafrost, while the region south of the line is essentially permafrost-
31 free.

1 **2.2 Terminology**

2 Estimating wetland CH₄ emissions over large scales requires accurately delineating the
3 wetland area over which CH₄ emissions can occur. Unfortunately, “wetland” definitions vary
4 within the scientific community (Mitsch and Gosselink, 2000). For the purposes of
5 estimating CH₄ emissions, the key characteristics include anoxia and available labile carbon
6 substrate; therefore we will adopt the definition proposed by Canada’s National Wetlands
7 Working Group (Tarnocai et al., 1988): land that is saturated with water long enough to
8 promote wetland or aquatic processes as indicated by poorly drained soils, hydrophytic
9 vegetation, and various kinds of biological activity which are adapted to a wet environment.
10 Because permanent, deep (> 2m) open water bodies are subject to additional processes (e.g.,
11 allocthonous carbon inputs, wind-driven mixing of the water column; Pace et al., 2004), we
12 will exclude them from our definition. Unfortunately, explicit observations of lake depths are
13 lacking for all but the deepest lakes; therefore we will instead use an area threshold (1 km²) to
14 identify permanent lakes. This definition of wetlands therefore includes all peatlands
15 (inundated or not), seasonally-inundated non-peatland soils (e.g., river floodplains), and small
16 ponds or lakes; but excludes rivers and large lakes.

17 We define “surface water” as all fresh water above the soil surface; i.e., the superset of
18 inundation, lakes, and rivers. We define “inundation” as temporary (present for less than 1
19 year) standing water above the soil surface; “lakes” as permanent water bodies (present for
20 more than 1 year) exceeding 1 km² in area; and “rivers” as channels that carry turbulent water.
21 Surface water therefore includes areas that do not emit large amounts of CH₄, such as rivers,
22 and also excludes some CH₄-emitting areas such as non-inundated peatlands.

23 For models, we will use the term “CH₄-producing area” to refer to the area over which CH₄
24 production is simulated, which might not coincide exactly with the areas of actual or
25 simulated wetlands.

26 **2.3 Observations and Inversions**

27 Table 1 lists the various observations and inversions that we used in this study. We
28 considered four wetland map products over the WSL, all of which have been used in high-
29 latitude wetland carbon studies. Two of them are regional maps specific to the WSL: Sheng
30 et al. (2004), denoted by “Sheng2004”; and Peregon et al. (2008), denoted by “Peregon2008”.
31 Both Sheng 2004 and Peregon2008 used the 1:2,500,000-scale map of Romanova (1977):

1 Peregon2008 was entirely based on the Romanova map, while Sheng2004 used the
2 Romanova map north of 65° N and used the 1:100,000-scale maps of Markov (1971) and
3 Matukhin and Danilov (2000) elsewhere. Both of these maps delineate the extents of
4 peatlands, including ponds and lakes smaller than 1km² in area. The Sheng2004 product
5 additionally includes a separate layer delineating lakes larger than 1km². The Peregon2008
6 product distinguishes between various wetland sub-types (e.g., sphagnum- or sedge-
7 dominated bogs, high palsa mires, etc.). The third map is the Northern Circumpolar Soil
8 Carbon Database (“NCSCD”; Tarnocai et al., 2009), an inventory of carbon-rich soils,
9 including peatlands, within the Arctic permafrost region. Models that have used this database
10 have taken the histel and histosol delineations to be synonymous with peatlands. The fourth
11 map is the wetland layer (GLWD-3, excluding the rivers and lakes of area > 1km² of layers
12 GLWD-1 and GLWD-2) of the Global Lake and Wetland Database (“GLWD”; Lehner and
13 Döll, 2004), in which wetland extents are the union of polygons from four different global
14 databases.

15 Two global time-varying surface water products derived from remote sensing observations
16 were also examined in this study: the Global Inundation Extent from Multi-Satellites
17 (“GIEMS”; Prigent et al., 2007; Papa et al., 2010), derived from visible/near-infrared
18 (AVHRR) and active (SSM/I) and passive (ERS) microwave sensors over the period 1993-
19 2004; and the Surface Water Microwave Product Series (“SWAMPS”; Schroeder et al.,
20 2010), derived from active (SeaWinds-on-QuikSCAT, ERS, and ASCAT) and passive
21 (SSM/I, SSMI/S, AMSR-E) microwave sensors over the period 1992-2013. For both
22 products, surface water area fractions (F_w) were aggregated from their native 25 km equal-
23 area grids to a 0.5×0.5° geographic grid and from daily to monthly temporal resolution, for
24 consistency with model results.

25 For CH₄ emissions, our primary reference for in situ observations was the estimate of
26 Glagolev et al. (2011), which we will refer to as “Glagolev2011”. The Glagolev2011 product
27 consists of both a database of over 2000 individual chamber observations from representative
28 landforms at each of 36 major sites over the period 2006-2010 (Figure 1a) and a map of long-
29 term average emissions created by applying the mean observed emissions to the wetlands of
30 the Peregon2008 map as a function of wetland type. It is worth noting that the Glagolev2011
31 product is currently undergoing a revision based on higher-resolution maps, which will lead to
32 a substantial increase in annual emissions from the Taiga zone, due to a larger spatial extent

1 of high-emitting wetland types (Glagolev et al., 2013). Possible changes to emissions in the
2 Tundra zone (in the northern half of the WSL) are not yet known. We consider this product's
3 large uncertainty in our evaluation of model predictions.

4 We also considered emissions estimates from five inversions. Two of them were regional:
5 "Kim2011" (Kim et al., 2011) and "Winderlich2012" (Winderlich, 2012; Schuldt et al.,
6 2013). Kim et al. (2011) used an earlier version of Glagolev2011 (Glagolev et al., 2010) at
7 $1\times 1^\circ$ resolution as their prior distribution for wetland emissions within the atmospheric
8 transport model NIES-TM (Maksyutov et al., 2008) over the period 2002-2007. Kim et al.
9 (2011) derived 12 climatological average monthly (spatially uniform) coefficients for wetland
10 emissions to optimize atmospheric CH_4 concentrations over the WSL relative to observed
11 CH_4 concentrations obtained by aircraft sampling at two locations in the WSL. Winderlich
12 (2012) used the Kaplan (2002) wetland inventory for prior wetland emissions, within the
13 global inversion system TM3-STILT (Rödenbeck et al., 2009; Trusilova et al., 2010) for the
14 year 2009. Winderlich (2012) derived 12 monthly coefficients for wetland emissions,
15 uniquely for each point in a $1\times 1^\circ$ grid, to optimize atmospheric CH_4 concentrations over the
16 WSL relative to the concentrations measured at the Zotino Tall Tower Observatory and three
17 other CH_4 tower observation sites (Demyanskoe, Igrim, and Karasevoe) located between 58
18 and 63°N .

19 The other inversions we considered were global: The "Reference" and "Kaplan" versions of
20 the Bousquet et al. (2011) inversion, denoted by "Bousquet2011R" and "Bousquet2011K",
21 respectively; and the estimate of Bloom et al. (2010), denoted by "Bloom2010". Bousquet et
22 al. (2011) used the LMDZ (Li, 1999) atmospheric transport model on a $3.75\times 2.5^\circ$ grid to
23 estimate monthly CH_4 emissions at $1\times 1^\circ$ resolution for the period 1993-2009, optimizing
24 atmospheric concentrations of several gases including CH_4 relative to global surface
25 observation networks, for both inversions. The Matthews and Fung (1987) emissions
26 inventory was the prior for wetland emissions in the Bousquet2011R inversion, while the
27 Kaplan (2002) emissions were the prior for the Bousquet2011K inversion. In both cases, a
28 single, spatially uniform set of monthly coefficients was derived for each of 11 large regions
29 of the globe. The region containing the WSL was Boreal Asia (in which the WSL makes up
30 the majority of the wetlands). Consequently, spatial patterns in estimated emissions at the
31 scale of $1\times 1^\circ$ were identical to those of the prior emissions; only the regional total emissions
32 were constrained by the inversions. The 17-year record length of the Bousquet2011

1 inversions made them appealing candidates for investigating the sensitivities of emissions to
2 interannual variability in environmental drivers. Bloom et al. (2010) did not use an
3 atmospheric transport model, but rather optimized the parameters in a simple model relating
4 observed atmospheric CH₄ concentrations from the Scanning Imaging Absorption
5 Spectrometer for Atmospheric Chemistry (SCIAMACHY; Bovensmann et al., 1999) on the
6 Envisat satellite to observed surface temperatures from the National Center for Environmental
7 Prediction/National Center for Atmospheric Research (NCEP/NCAR) weather analyses
8 (Kalnay et al., 1996) and gravity anomalies from the Gravity Recovery and Climate
9 Experiment satellite (GRACE; Tapley et al., 2004), under the assumption that gravity
10 anomalies are indicative of large-scale surface and near-surface water anomalies. The
11 Bloom2010 inversion covered the period 2003-2007, at 3×3 degree resolution.

12 **2.4 Models**

13 Among the participating models (Table 2) were those of the WETCHIMP study (Melton et
14 al., 2013; Wania et al., 2013) that contributed CH₄ emissions estimates: CLM4Me (Riley et
15 al., 2011), DLEM (Tian et al., 2010, 2011a,b, 2012), IAP-RAS (Mokhov et al., 2007; Eliseev
16 et al., 2008), LPJ-Bern (Spahni et al., 2011, Zürcher et al., 2013), LPJ-WHyMe (Wania et al.,
17 2009a,b; Wania et al., 2010), LPJ-WSL (Hodson et al., 2011), ORCHIDEE (Ringeval et al.,
18 2010), SDGVM (Hopcroft et al., 2011), and UW-VIC (denoted by “UW-VIC (GIEMS)”;
19 Bohn et al., 2013). In addition, we analyzed several other models. “UW-VIC (SWAMPS)” is
20 another instance of UW-VIC with surface water calibrated to match the SWAMPS product.
21 VISIT (Ito and Inatomi, 2012), contributed four configurations using different combinations
22 of wetland maps and methane models: “VISIT (GLWD)” and “VISIT (Sheng)” used the Cao
23 (1996) methane model with the GLWD and Sheng2004 wetland maps, respectively, and
24 “VISIT (GLWD-WH)” and “VISIT (Sheng-WH)” replaced the Cao model with the Walter
25 and Heimann (2000) model. LPX-BERN (Spahni et al., 2013; Stocker et al., 2013, 2014) is a
26 newer version of LPJ-Bern that also contributed four configurations: “LPX-BERN”, which
27 prescribed peatland extent using Peregon2008 and inundation extent using GIEMS; “LPX-
28 BERN (DYPTOP)”, which dynamically predicted the extents of peatlands and inundation;
29 and “LPX-BERN (N)” and “LPX-BERN (DYPTOP-N)”, which additionally simulated
30 interactions between the carbon and nitrogen cycles. DLEM2 is a newer version of DLEM
31 that includes soil thermal physics and lateral matter fluxes (Liu et al. 2013, Pan et al. 2014).
32 LPJ-MPI (Kleinen et al., 2012) is a version of the LPJ model that contains a dynamic peatland

1 model with methane transport by the model of Walter and Heimann (2000). Finally, VIC-
2 TEM-TOPMODEL (Zhu et al., 2014) is a hybrid of UW-VIC (Liang et al., 1994), TEM
3 (Zhuang et al., 2004), and TOPMODEL (Beven and Kirkby, 1979).

4 The relevant hydrologic and biogeochemical features of these models are listed in Tables 2
5 and 3, respectively. The models used a variety of approaches to define CH₄-producing areas.
6 To have some consistency across models, the original WETCHIMP study asked participating
7 modelers to use the GIEMS product if their model required wetland extent to be prescribed.
8 Accordingly, some models (DLEM, DLEM2, and LPJ-WSL) used the GIEMS surface water
9 product exclusively to prescribe (time-varying) CH₄-producing areas; these are denoted with
10 the code “S” in Table 2.

11 Several models (CLM4Me, LPJ-MPI, LPX-BERN (DYPTOP), LPX-BERN (DYPTOP-N),
12 ORCHIDEE, SDGVM, and VIC-TEM-TOPMODEL) predicted surface water and CH₄-
13 producing areas dynamically using topographic information and the TOPMODEL (Beven and
14 Kirkby, 1979) distributed water table approach (in which the area over which the water table
15 is at or above the soil surface can be interpreted to correspond to surface water extent); these
16 models are denoted with a “T” in Table 2. For these models, the CH₄-producing area is the
17 area in which labile soil carbon is sufficiently warm and anoxic for methanogenesis to occur,
18 including both surface water and any non-inundated land with sufficiently shallow water table
19 depths. LPJ-MPI and LPX-BERN (DYPTOP and DYPTOP-N) prognostically determined
20 peatland area as a function of long-term soil moisture conditions; their CH₄-producing areas
21 thus included peatlands (inundated or not) as well as completely saturated or inundated
22 mineral soils. Because the other “T” models’ CH₄-producing areas had no explicit limits,
23 those teams reported approximations of the models’ true CH₄-producing areas: CLM4Me,
24 ORCHIDEE, and VIC-TEM-TOPMODEL reported their surface water areas; and SDGVM
25 reported the area for which the water table was above a threshold depth, with the threshold
26 chosen to minimize the global RMS error between this area and GIEMS. Additionally, both
27 CLM4Me and ORCHIDEE tied their surface water areas to the long-term mean of GIEMS:
28 CLM4Me did so by calibration and ORCHIDEE did so by rescaling its surface water areas.
29 Thus, we have placed these two models in the “S” category in Table 2.

30 Finally, the remaining models (IAP-RAS, LPJ-Bern, LPJ-WHyMe, LPX-BERN, LPX-BERN
31 (N), both UW-VIC configurations, and all four VISIT configurations) used wetland maps,
32 either alone or in combination with topography and surface water products, to inform their

1 wetland schemes; these are denoted with “M” in Table 2. In most cases, the wetland maps
2 were used to determine the maximum extent of the CH₄-producing area, within which
3 inundated area and water table depths would vary in time. In contrast, LPJ-Bern, LPX-
4 BERN, and LPX-BERN (N) allowed inundated area (specified by GIEMS) to sometimes
5 exceed the static map-based peatland area; in such cases, it was assumed that the excess
6 inundation occurred in mineral soils. Thus, the CH₄-producing area included peatlands and
7 inundated mineral soils. LPJ-Bern additionally allowed CH₄ production in areas of “wet
8 mineral soil” (in which soil moisture content was greater than 95% of water holding capacity)
9 and included this in the total CH₄-producing area.

10 Models’ hydrologic approaches varied in other ways as well. Some (IAP-RAS and LPJ-
11 WSL) did not include explicit water table depth formulations for estimating emissions in
12 unsaturated (non-inundated) wetlands; IAP-RAS assumed all wetlands were completely
13 saturated and LPJ-WSL only considered unsaturated wetlands implicitly, using soil moisture
14 as a proxy. Most of the other models used a TOPMODEL approach to relate the distribution
15 of water table depths across the grid cell to topography (generally at 1-km scale). However,
16 LPJ-WHyMe, UW-VIC (GIEMS) and UW-VIC (SWAMPS) determined water table depth
17 distributions within peatlands from assumed proportions of microtopographic landforms (e.g.,
18 hummocks and lawns) at the (horizontal) scale of meters. UW-VIC explicitly handled
19 lakes by treating lakes and peatlands as a single system, spanning the total area of lakes and
20 peatlands given by the Sheng et al. (2004) dataset and within which surface water area varied
21 dynamically. Areas of permanent surface water over the period 1949-2010 were considered
22 to be lakes, and excluded from methane emissions estimates.

23 Models also varied in their soil thermal physics schemes. Most models used a 1-dimensional
24 heat diffusion scheme to determine the vertical profile of soil temperatures, but VISIT used a
25 linear interpolation between current air temperature (at the soil surface) and annual average
26 air temperature (at the bottom of the soil column). Several models (DLEM, LPJ-MPI, LPJ-
27 WSL, and SDGVM) did not consider the water-ice phase change and therefore did not model
28 permafrost. While IAP-RAS contained a permafrost scheme, it was driven by seasonal and
29 annual summaries of meteorological forcings and used simple analytic functions to estimate
30 the seasonal evolution and vertical profile of soil temperatures. Additionally, DLEM and
31 LPJ-WSL did not consider the insulating effects of organic (peat) soil. In contrast, UW-VIC

1 modeled permafrost, peat soils, and the dynamics of surface water, including lake ice cover
2 and evaporation, thereby adding another factor that influences soil temperatures.

3 Models also varied in their biogeochemical schemes (Table 3). Most represented methane
4 production as a function of soil temperature, water table depth (except for IAP-RAS and LPJ-
5 WSL), and the availability of carbon substrate. Most (except for IAP-RAS and LPJ-WSL)
6 explicitly accounted for oxidation of methane above the water table; and most accounted for
7 some degree of plant-aided transport. Some models (LPJ-Bern, LPJ-MPI, LPJ-WHyMe, and
8 LPX-BERN) represented methane production as either a constant or soil-moisture-dependent
9 fraction of aerobic respiration. Some models (DLEM, DLEM2, and VIC-TEM-
10 TOPMODEL) imposed additional dependences on soil pH and oxidation state. Models
11 differed in the pathways and availability of carbon substrate: some models (UW-VIC, VIC-
12 TEM-TOPMODEL, VISIT (GLWD-WH) and VISIT (Sheng-WH)) related carbon substrate
13 availability to net primary productivity (NPP) as a proxy for root exudates; others (CLM4Me,
14 IAP-RAS, LPJ-MPI, LPJ-WSL, ORCHIDEE, SDGVM, VISIT (GLWD) and VISIT (Sheng))
15 related carbon substrate to the content and residence times of various soil carbon reservoirs;
16 and others (DLEM, DLEM2, LPJ-Bern, LPJ-WHyMe, all four LPX-BERN configurations)
17 drew carbon substrate from a combination of both root exudates and soil carbon (or dissolved
18 organic carbon, in the case of DLEM and DLEM2). CLM4Me and two configurations of
19 LPX-BERN simulated interactions between the carbon and nitrogen cycles. Several models
20 (all versions of LPJ and LPX, ORCHIDEE, and SDGVM) included dynamic vegetation
21 components. Some models (LPJ-Bern, LPJ-MPI, LPJ-WHyMe, LPX-BERN, and UW-VIC)
22 accounted for inhibition of NPP of some plant species under saturated soil moisture
23 conditions. Finally, models employed a variety of methods, alone or in combination (Table
24 3), to select parameter values, including: taking the median of literature values; optimizing
25 emissions to match in situ observations from representative sites regionally (e.g., UW-VIC
26 optimized parameter values to match the Glagolev2011 dataset in the WSL) or globally; or
27 optimizing global total emissions to match various estimates from inversions.

28 **2.5 Model Simulations**

29 To be consistent with WETCHIMP's transient simulation ("Experiment 2-trans", Wania et al.,
30 2013), we focused our analysis on the period 1993-2004, although several non-WETCHIMP
31 models provided data from 1993 to 2010. All models used the CRUNCEP gridded

1 meteorological forcings (Viovy and Ciais, 2011) as a common input. Model-specific inputs
2 are described in Wania et al. (2013).

3 Model outputs (monthly CH₄ emissions (average g CH₄ month⁻¹ m⁻² over the grid cell area)
4 and monthly CH₄-producing area (km²)) were analyzed at 0.5×0.5 degree spatial resolution
5 (resampled from native resolution as necessary).

6 Due to large seasonal variations in CH₄-producing areas, our analysis focused on June-July-
7 August (JJA) averages of area and CH₄ emissions, since it is during these months that the
8 majority of the year's methane is emitted, across all models (areas from other seasons would
9 not be representative of CH₄ emissions). Similarly, in analyzing interannual variability in
10 CH₄ emissions, we focused on JJA CH₄ emissions, which dominate the annual total and have
11 stronger correlations with JJA environmental factors (such as air temperature, precipitation, or
12 inundation) than annual CH₄ emissions have with annual average environmental factors. We
13 also computed growing season CH₄ “intensities” (average JJA CH₄ emissions per unit JJA
14 CH₄-producing area).

15 **2.6 Data Access**

16 All data used in this study, including observational products, inversions, and forward model
17 results, are available from WETCHIMP-WSL (2015).

18

19 **3 Results**

20 **3.1 Average Annual Total Emissions**

21 As shown in Figure 2 and Table S1, 12-year mean estimates (\pm standard error on the mean) of
22 annual total emissions over the WSL from forward models (5.34 ± 0.54 Tg CH₄ y⁻¹),
23 inversions (6.06 ± 1.22 Tg CH₄ y⁻¹), and observations (3.91 ± 1.29 Tg CH₄ y⁻¹) largely agreed,
24 despite large scatter in individual estimates. Model estimates ranged from 2.42 Tg CH₄ y⁻¹
25 (LPX-BERN (DYPTOP-N)) to 11.19 Tg CH₄ y⁻¹ (IAP-RAS). The Glagolev2011 estimate
26 was substantially lower than the mean of the models, corresponding to the 36th percentile of
27 the distribution of model estimates. However, the potential upward revision of Glagolev2011
28 (Section 2.2) would move it to a substantially higher percentile of their distribution.
29 Inversions yielded a similarly large range of estimates, 3.08 Tg CH₄ y⁻¹ (Kim2011) to 9.80 Tg

1 CH₄ y⁻¹ (Winderlich2012). Despite their large spread, 15 out of the 17 forward models fell
2 within the range of inversion estimates. Here we have excluded the “WH” configurations of
3 VISIT and the configurations of LPX-BERN for which nitrogen-carbon interaction was
4 turned off, due to their similarities to their counterparts that were included. The wide variety
5 in the relative proportions of CH₄ emitted from the South and North halves of the domain,
6 with the Southern contribution ranging from 13% to 69% (right-hand column in Figure 2),
7 indicates lack of agreement on which types of wetlands and climate conditions are producing
8 the bulk of the region’s CH₄.

9 **3.2 Differences Among Observational Datasets**

10 The large degree of disagreement among observational datasets is worth addressing before
11 using them to evaluate the models. Important differences are evident among wetland maps
12 (Figure 3). Sheng2004 and Peregon2008 are extremely similar, in part because they both
13 used the map of Romanova (1977) north of 65° N. Both of these datasets show wetlands
14 distributed across most of the WSL, with large concentrations south of the Ob’ River (55-61°
15 N, 70-85° E), east of the confluence of the Ob’ and Irtysh Rivers (57-62° N, 65-70° E) and
16 north of the Ob’ River (61-66° N, 70-80° E). In comparison, the GLWD map entirely lacks
17 wetlands in the tundra region north of 67° N and shows additional wetland area in the north-
18 east (64-67° N, 70-90° E). The NCSCD is substantially different from the other three maps.
19 Owing to its focus on permafrost soils, it completely excludes the extensive wetlands south of
20 the southern limit of permafrost (approximately 60° N). Given the numerous field studies
21 documenting these productive southern wetlands (Section 2.1), the NCSCD seems to be
22 inappropriate for studies that extend beyond permafrost.

23 The two surface water products (GIEMS and SWAMPS) also exhibit large differences.
24 While they both agree that the surface water area fraction (F_w) is most extensive in the central
25 region north of the Ob’ River (61-64° N), GIEMS gives areal extents that are 3-6 times those
26 of SWAMPS. Outside of this central peak, GIEMS F_w drops off rapidly to nearly 0 in most
27 places (particularly in the forested region south of the Ob’ River, which may be due to
28 difficulties in detecting inundation under vegetative canopy and/or reduced sensitivity where
29 open water fraction is less than 10 %; Prigent et al. 2007), while SWAMPS maintains low
30 levels of F_w throughout most of the WSL. Along the Arctic coastline, SWAMPS shows high
31 F_w , which may indicate contamination of the signal by the ocean. In both datasets, F_w

1 exhibits some similarity with the distribution of lakes and rivers (Figure 1), illustrating the
2 inclusion of non-wetlands in these surface water products.

3 Among the CH₄ datasets (Figure 4), a clear difference can be seen between the spatial
4 distributions of Glagolev2011 and Kim2011 (both of which assign the majority of emissions
5 to the region south of the Ob' River, between 55 and 60° N); and Winderlich2012 and
6 Bousquet2011K (both of which assign the majority of emissions to the central region north of
7 the Ob' River, between 60 and 65° N). We discuss possible reasons for this discrepancy in
8 Section 4.3. The global inversions (Bousquet2011R and K, and Bloom2010) have coarser
9 spatial resolution than the regional inversions of Kim2011 and Winderlich2012.

10 Bousquet2011R and K have similar distributions between 60 and 65° N, but Bousquet2011R
11 has relatively stronger emissions between 57 and 60° N and weaker emissions between 65 and
12 67° N; in this respect, Bousquet2011R is intermediate between Glagolev2011 and
13 Winderlich2012. Finally, Bloom2010 exhibits relatively little spatial variability in emissions,
14 likely due to its use of GRACE observations as a proxy for wetland inundation and water
15 table conditions.

16 **3.3 Primary Drivers of Model Spatial Uncertainty**

17 The wide disagreement among models is plainly evident in Figure 5, which plots average JJA
18 CH₄ emissions versus average JJA CH₄-producing areas for the WSL as a whole (top left), the
19 South (bottom left), and the North (bottom right). A series of lines (“spokes”) passing
20 through the origin, with slopes of integer multiples of 1 g CH₄ m⁻² mon⁻¹, allows comparison
21 of spatial average intensities (CH₄ emissions per unit CH₄-producing area). All points along a
22 given line have the same intensity but different CH₄-producing areas. We have included the
23 Glagolev2011/Peregon2008 CH₄ /area estimate (denoted by a black star) and the mean of the
24 inversions (denoted by a grey star) for reference. We set the area coordinate for the
25 inversions to Peregon2008, because a) the wetland area was not available for all inversions,
26 and b) Peregon2008 is a relatively accurate estimate of wetland area. JJA CH₄ emissions,
27 JJA wetland or CH₄-producing areas, and JJA intensities, for all models, observations, and
28 inversions, are listed in Table S1. Over the entire WSL (Figure 5, top left), the scatter in
29 model estimates of CH₄ emissions results from scatter in both area (ranging from 200,000 to
30 1,200,000 km²) and intensity (ranging from 1 to 8 g CH₄ m⁻² mon⁻¹), with no clear
31 relationship between the two.

1 However, a strong area-driven bias is evident in the South (Figure 5, bottom left). Although
2 the mean modeled CH₄ emission rate (0.58 Tg CH₄ mon⁻¹) is fairly close to both
3 Glagolev2011 (0.67 TgCH₄ mon⁻¹) and the mean of inversions (0.60 Tg CH₄ mon⁻¹), the
4 distribution of model estimates is substantially skewed, with most models' estimates falling
5 well below both Glagolev2011 and the mean of the inversions. Glagolev2011's estimate
6 corresponds to the 81st percentile of the model CH₄ distribution; the expected upward revision
7 of Glagolev2011 (Section 2.2; exact JJA amount not yet known) would only raise that
8 percentile. The mean of the inversions corresponds to the 76th percentile. Similarly, the
9 models substantially underestimate CH₄-producing area, with Peregon2008 occupying the
10 83rd percentile of the model distribution. On the other hand, the model intensity distribution
11 is much less biased, with Glagolev2011 corresponding to the 47th percentile. Even a doubling
12 of Glagolev2011's intensity would place it at only the 69th percentile of the model
13 distribution, a smaller bias than for area. Thus, the area bias is the major driver of CH₄ bias in
14 the South. In comparison, the North (Figure 5, bottom right) is relatively unbiased.

15 Model inputs and formulations played a key role in determining CH₄-producing area biases.
16 Statistics of model performance relative to Glagolev2011/Peregon2008, categorized by the
17 wetland codes in Table 2, are listed in Table 4. The models that used satellite surface water
18 products alone (denoted with circles in Figure 5 and the code "S" in Table 2) estimated the
19 lowest CH₄-producing areas in the South, with a bias of -270,000 km² and standard deviation
20 of 31,000 km². Additionally, two models (LPJ-Bern and LPJ-WHyMe) from the "M" group
21 (denoted by squares in Figure 5 and the code "M" in Table 2) also yielded low areas, due to
22 their use of the NCSCD map, which omitted non-permafrost wetlands. The "M+" group,
23 consisting of all "M" models except those two, exhibited the smallest bias and second-
24 smallest standard deviation (-31,000 km² and 34,000km², respectively). Models that
25 determined CH₄-producing area dynamically using topographic data, but without the
26 additional input of wetland maps (denoted by triangles in Figure 5 and the code "T" in Table
27 2) yielded nearly as small a bias as the "M+" group (-42,000 km²), but had the largest scatter
28 (standard deviation of 173,000 km²) of the groups. The fact that two of the "S" models
29 (CLM4Me and ORCHIDEE) supplied CH₄-producing areas that excluded non-inundated
30 methane-emitting wetlands had little effect on the results, since their total CH₄ emissions
31 (which included non-inundated emissions) also suffered from a large negative bias (-0.45 Tg
32 CH₄ y⁻¹, or -67%).

1 Examining the spatial distributions of annual CH₄ (Figure 6) and JJA CH₄-producing areas
2 (Figure 7) shows why the use of surface water data alone results in poor model performance.
3 Among the models from the “S” group (CLM4Me, DLEM, DLEM2, LPJ-WSL, and
4 ORCHIDEE), the spatial distributions of both CH₄ emissions and CH₄-producing area tend to
5 be strongly correlated with GIEMS (See Table 5 for correlations), which exhibits very low
6 surface water areas south of the Ob’ River, despite the large expanses of wetlands there
7 (section 3.2). Similarly, the low emissions of LPJ-WHyMe and LPJ-Bern in the South can be
8 explained by their use of the NCSCD map, which only considered peatlands (histels and
9 histosols) within the circumpolar permafrost zones (which only occur north of 60° N). For
10 LPJ-WHyMe, these permafrost peatlands were the only type of wetland modeled (i.e., the
11 model domain only included the circumpolar permafrost zones), so LPJ-WHyMe’s emissions
12 were almost nonexistent in the South. LPJ-Bern also used the NCSCD’s histels and histosols
13 to delineate peatlands, but additionally simulated methane dynamics in wet or inundated
14 mineral soils outside the permafrost zone. While this allowed LPJ-Bern to make emissions
15 estimates in the South, the much lower porosities of mineral soils resulted in larger
16 sensitivities of water table depth to evaporative loss than those of peat soils. These drier soils
17 led to net CH₄ oxidation in much of the South.

18 Aside from area-driven biases, a large degree of intensity-driven scatter is evident in both the
19 South and North. Indeed, the underestimation of areas in the South, accompanied by resulting
20 reductions in CH₄ emissions, partially compensated for some of the intensity-driven scatter
21 there. However, some of the more extreme intensities were arguably the result of area biases,
22 in that some of the global wetland models (CLM4Me, IAP-RAS, LPJ-Bern, and LPJ-
23 WHyMe) scaled their intensities to match their global total emissions with those of global
24 inversions, which could result in local biases if their wetland maps suffered from either global
25 or local bias (which was true of these models). Interestingly, several models yielded
26 estimates similar to those of the two regionally-optimized UW-VIC simulations, implying that
27 the regional optimization did not confer a distinct advantage on UW-VIC.

28 Nitrogen limitation influenced intensity in LPX-BERN, the one model that included it.
29 Although we did not plot results from the two LPX-BERN configurations that lacked
30 nitrogen-carbon interactions in Figure 5, we compare results from all four LPX-BERN
31 configurations in Table 6. In LPX-BERN (N) and LPX-BERN (DYPTOP-N), the nitrogen
32 limitation imposed by nitrogen-carbon interactions substantially reduced NPP, relative to

1 LPX-BERN and LPX-BERN (DYPTOP), leading to a reduction of mean annual CH₄
2 emissions of approximately 20% over the entire WSL over the period 1993-2010. This
3 reduction was slightly larger than the difference in emissions between simulations using the
4 Sheng2004 map to prescribe peatland area (LPX-BERN and LPX-BERN (N)) and
5 simulations using the DYPTOP method to determine peatland extent dynamically (LPX-
6 BERN (DYPTOP) and LPX-BERN (DYPTOP-N)). In addition, the reduction in emissions
7 due to nitrogen limitation was concentrated in the northern half of the domain, in contrast to
8 the reduction due to dynamic peatland extent, which was concentrated in the southern half of
9 the domain. Nitrogen limitation also reduced trends in CH₄ emissions over the entire WSL
10 over the period 1993-2010, through reductions in soil carbon accumulation rates. However,
11 both these trends and their reductions were very small (< 0.5% per year in most cases) and
12 statistically insignificant over the study period.

13

14 **3.4 Model Temporal Uncertainty and Major Environmental Drivers**

15 **3.4.1 Average Seasonal Cycles**

16 Models demonstrated general agreement on the shape of the seasonal cycle of emissions
17 (Figure 8, top left) and intensities (Figure 8, bottom right), despite wide disagreement on the
18 shape and timing of the seasonal cycle of CH₄-producing area (Figure 8, bottom left). The
19 regional inversions (Kim2011 and Winderlich2012) agreed on a July peak for CH₄, although
20 Winderlich2012 suggested a noticeably larger contribution from cold season months than the
21 others (which is plausible, given reports of non-zero winter emissions; Rinne et al., 2007;
22 Kim et al., 2007; Panikov and Dedysh, 2000). In contrast, both Bousquet inversions peaked
23 in August. Unlike the other three inversions, the Bousquet2011R inversion had negative
24 emissions (net oxidation) in either May or June of almost every year of its record. These
25 negative emissions were widespread, throughout not only the WSL but the entire Boreal Asia
26 region, and cast doubt on the accuracy of their seasonal cycle. Turning to the surface water
27 products (Figure 8, bottom left), GIEMS and SWAMPS displayed quite different shapes in
28 their seasonal cycles of surface water extent: GIEMS exhibited a sharp peak in June and
29 SWAMPS displayed a broad, flat maximum from June through September. In fact,

1 SWAMPS had a similar shape to GIEMS south of about 64° N; the broad peak for the WSL
2 as a whole was the result of late-season peaks further north.

3 Most models' CH₄ emissions peaked in July, in agreement with the regional inversions. A
4 few models peaked in June: CLM4Me, DLEM2, LPJ-MPI, VISIT (GLWD) and VISIT
5 (Sheng). Correspondingly early peaks in intensity can explain the early peaks in the DLEM2
6 and the VISIT simulations, indicating either early availability of carbon substrate in the soil or
7 rapid soil warming (the latter is likely for VISIT, given its linearly-interpolated soil
8 temperatures). In contrast, LPJ-MPI's early peak in emissions was the result of an early
9 (May) peak in CH₄-producing area, which, in turn, was the result of early snow melt. Two
10 models (LPJ-BERN and UW-VIC (GIEMS)) peaked in August. LPJ-Bern's late peak
11 resulted from a late peak in wet mineral soil intensity, despite an exceptionally late (October)
12 peak in CH₄-producing area. The late peak of UW-VIC (GIEMS) corresponded to a late peak
13 in intensity, implying either late availability of carbon substrate (due to inhibition of NPP
14 under inundation) or delayed warming of the soil (due to excessive insulation by peat or
15 surface water).

16 Aside from the above cases, the relative agreement among models on a July peak in CH₄
17 emissions comes despite wide variation in seasonal cycles of CH₄-producing area. For
18 example, DLEM's CH₄-producing area held steady at its maximum extent from April through
19 November; and VIC-TEM-TOPMODEL's CH₄-producing area peaked in August, possibly
20 due to low evapotranspiration or runoff rates. Some of the discrepancies in CH₄-producing
21 area seasonality arose from several models' using static maps to define some or all wetland
22 areas (Sections 2.3 and 2.4). These differences matter little to the seasonal cycle of CH₄
23 emissions, in part because of the similarity between the seasonal cycles of inundated area and
24 water table depths within the static CH₄-producing areas, and in part because of the nearly
25 universal strong correlation at seasonal time scales between simulated intensities and near-
26 surface air temperature (so that cold-season CH₄-producing areas have little influence over
27 emissions).

28 **3.4.2 Interannual Variability**

29 At multi-year time scales (shown for the period 1993-2010 in Figure 9), models' and
30 inversions' total annual CH₄ emissions displayed a wide range of interannual variability, even
31 after accounting for the effects of differences in intensity. Values of the coefficient of

1 variation (CV) for models over the period 1993-2004 ranged from 0.069 (LPX-BERN (N)) to
2 0.338 (UW-VIC (GIEMS)) with a mean of 0.169 (Table 7). While Bousquet2011K's CV of
3 0.160 fell near the mean model CV, Bousquet2011R's CV of 0.446 was 25% larger than the
4 largest model CV, and over twice the second-largest model CV. Bousquet2011R's high
5 variability was due in part to a peak in CH₄ emissions in 2002 followed by a large drop in
6 emissions between 2002 and 2004, actually becoming negative (net CH₄ oxidation) in 2004
7 before continuing at a much lower mean value from 2005 to 2009. This peak and decline
8 coincide with a similar peak and decline in F_w (Figure 10) and precipitation (Figure 11).
9 Several models (notably LPJ-MPI, LPJ-WHyMe, LPJ-WSL, DLEM, and VIC-TEM-
10 TOPMODEL), as well as Bousquet2011K, mirrored this drop to varying degrees, but none
11 dropped as much in proportion to their means or became negative. In contrast, Bloom2010,
12 spanning only the period 2003-2007, exhibited extremely little interannual variability, perhaps
13 due to its use of GRACE as a proxy for inundated area and water table depth.

14 To investigate the influence of various climate drivers on CH₄ emissions, we computed the
15 individual correlations between the JJA CH₄ emissions and the following JJA drivers: CRU
16 air temperature (T_{air}), CRU precipitation (P), GIEMS F_w, and SWAMPS F_w, for forward
17 models and the two Bousquet2011 inversions, over the period 1993-2004 (Table S2). Here
18 we included four additional model configurations that we did not show in previous sections:
19 VISIT (GIEMS-WH), VISIT (SHENG-WH), LPX-BERN, and LPX-BERN-DYPTOP. The
20 two drivers yielding the highest correlations with JJA CH₄ emissions were JJA CRU T_{air} and
21 JJA GIEMS F_w. These two drivers also exhibited nearly zero correlation with each other over
22 the WSL and the South and North halves (Table 8). Because variations in water table
23 position are driven by the same hydrologic factors (snowmelt, rainfall, evapotranspiration,
24 and drainage) that drive variations in F_w, correlation with F_w should serve as a general
25 measure of the influence of both surface and subsurface moisture conditions on methane
26 emissions, even for models that were not explicitly driven by F_w. Therefore, we chose to
27 examine model behavior in terms of correlations with JJA CRU T_{air} and JJA GIEMS F_w. As
28 an aside, this choice was not an endorsement of GIEMS over SWAMPS (which yielded
29 qualitatively similar results to GIEMS); it simply resulted in better separation among models.

30 The relative strengths of the correlations between models' CH₄ emissions and drivers varied
31 widely, as shown in the scatter plots in Figure 12. Over the entire WSL (top left) as well as
32 the South and North halves (bottom left and right), the low correlation between T_{air} and F_w led

1 to consistent trade-offs in the correlations between simulated emissions and T_{air} (x-axis) or F_w
2 (y-axis). Some models (all four LPX-BERN simulations, all four VISIT simulations, IAP-
3 RAS, ORCHIDEE, and SDGVM) had correlations with T_{air} that were greater than 0.7 in one
4 or both halves of the domain; since this means that T_{air} would explain the majority of CH_4
5 variance in a linear model, we have denoted them as “ T_{air} -dominated”. Other models (DLEM,
6 LPJ-WSL, DLEM2 and LPJ-MPI) were “ F_w -dominated” in one or both halves of the domain.
7 For the other models and inversions, no driver explained the majority of the variance. A few
8 models had small enough contributions from one or the other driver that the resulting
9 correlations were negative, due to the small negative correlation between T_{air} and F_w . Neither
10 of the two Bousquet2011 inversions exhibited strong correlations with either F_w or T_{air} , which
11 might imply that models also should not exhibit strong correlations with one driver.

12 Indeed, the overarching pattern in the model correlations was that models that lacked physical
13 and biochemical formulations appropriate to the high latitudes exhibited stronger correlations
14 with inundation or air temperature than either the inversions or more sophisticated models.
15 One characteristic that most of the F_w -dominated models (except for DLEM2) have in
16 common is that they lack soil thermal formulations that account for soil freeze/thaw
17 processes; conversely, most of the non- F_w -dominated models do have such formulations. In
18 addition, inundated fractions of DLEM, DLEM2, and LPJ-WSL were explicitly driven by
19 GIEMS F_w . Unlike the other three models, LPJ-MPI does account for the thermal effects of
20 peat soils, which might explain LPJ-MPI’s low (slightly negative) correlation with air
21 temperature.

22 Some of the T_{air} -dominated models also lack sophisticated soil thermal physics. VISIT’s
23 strong correlation with T_{air} can be explained by the fact that its soil temperature scheme is a
24 simple linear interpolation between current air temperature at the surface and annual average
25 air temperature at the bottom of the soil column; as a result, VISIT’s soil temperature has a
26 1.0 correlation with air temperature. Comparing the “WH” configurations of VISIT to the
27 default configurations, the model of Walter and Heimann (2000) had a lower correlation with
28 air temperature than the Cao (1996) model. SDGVM also lacks soil freeze-thaw dynamics.
29 IAP-RAS assumes all wetlands are completely saturated and holds their areas constant in
30 time; as a result, its CH_4 emissions have no dependence on soil moisture or F_w , but strong
31 dependence on air temperature. LPX-BERN’s high correlation with air temperature is the
32 result of a relative insensitivity of CH_4 emissions to water table depth, but at present there are

1 too few sites with multi-year observations in the region to determine whether this low
2 sensitivity is reasonable. Nitrogen-carbon interaction (LPX-BERN (N) and LPX-BERN
3 (DYPTOP-N)) appeared to have only a minor effect on LPX-BERN's interannual variability
4 in the North but led to a slight reduction in correlation with T_{air} in the South. Finally, UW-VIC
5 (GIEMS) had small negative correlations with both T_{air} and F_w in the North, likely the result
6 of its surface water formulation. UW-VIC's surface water dynamics had been initially
7 calibrated using the SWAMPS product; the much larger surface water extents of GIEMS in
8 the North resulted in substantially deeper surface water, with corresponding insulating effects,
9 greater evaporative cooling, and longer residence times, thus lowering correlations with both
10 observed F_w and T_{air} . The large difference in behavior between UW-VIC (GIEMS) and UW-
11 VIC (SWAMPS) implies that the differences arising from optimizing surface water dynamics
12 to different products far outweighed the differences between UW-VIC and other models in
13 their selection of biogeochemical parameters.

14 **4 Discussion**

15 **4.1 Long-Term Means and Spatial Distributions**

16 The most striking finding, in terms of long-term means and spatial distributions, was the
17 substantial bias in CH_4 emissions that resulted from using satellite surface water products or
18 inaccurate wetland maps to delineate wetlands. Surface water is an important component of
19 wetland models, but it clearly is a poor proxy for wetland extent at high latitudes, because it
20 both excludes the large expanses of strongly-emitting non-inundated peatlands that exist there
21 (Section 2.1) that were missed by GIEMS and underrepresented by SWAMPS; and
22 erroneously includes the high concentrations of large lakes there (e.g., Lehner and Döll,
23 2004), which do not necessarily emit methane at the same rates or via the same carbon
24 cycling processes as wetlands (e.g., Walter et al., 2006; Pace et al., 2004). The practical
25 difficulties in detecting inundation under forest canopies with visible or high-frequency
26 microwave sensors (e.g., Sippel and Hamilton, 1994) compound these problems. In the case
27 of the WSL, equating wetlands with surface water not only caused underestimation of total
28 CH_4 emissions, but also led to attribution of the majority of the region's emissions to the
29 permafrost zone in the North. This issue is not unique to the WSL, as the collocation of
30 permafrost, lakes, and inundation is present throughout the high latitudes (Tarnocai et al.,
31 2009; Lehner and Döll, 2004; Brown et al., 1998). Indeed, in their analysis of the Hudson
32 Bay Lowland (HBL), Melton et al. (2013) found that three of the four lowest emissions

1 estimates were from “S” models (CLM4Me, DLEM, and LPJ-WSL), although whether this
2 was due to a bias in area was not examined. Given present concerns over the potential
3 liberation of labile carbon from thawing permafrost over the next century (Koven et al.,
4 2011), it is crucial to avoid under- or over-estimating emissions from permafrost wetlands.

5 It is therefore important for modelers – both forward and inverse - to use accurate wetland
6 maps such as Peregon et al. (2008), Sheng et al. (2004), or Lehner and Döll (2004) in their
7 model development, whether as a static input parameter or as a reference for evaluating
8 prognostically-computed CH₄-producing areas; and to account for the existence of non-
9 inundated portions within these wetlands in which methane emissions have a dependence on
10 water table depth. Maps such as Tarnocai et al. (2009) may be inappropriate unless restricting
11 simulations to permafrost wetlands. Ideally, modelers would be able to draw on a global
12 version of the high-resolution map of Peregon et al (2008) that not only delineates wetlands,
13 but also identifies the major sub-types (e.g., sphagnum-dominated or sedge-dominated, as in
14 Lupascu et al., 2012) to which different methane emissions parameters could potentially be
15 applied. When using surface water products to constrain simulated inundated extents,
16 modelers must be sure either to mask out permanent lakes and large rivers, using a dataset
17 such as GLWD (Lehner and Döll, 2004) or MOD44W (Carroll et al. 2009); or better, to
18 implement carbon cycling processes that are appropriate to these forms of surface water.

19 **4.2 Temporal Variability, Environmental Drivers, and Model Features**

20 Another notable finding was that models that lacked physical and biochemical formulations
21 appropriate to the high latitudes exhibited more extreme correlations with F_w or air
22 temperature than either inversions or more sophisticated models. In other words, high-
23 latitude biogeophysical processes - specifically, soil freeze/thaw, the insulating effects of
24 snow and peat, and relationships between emissions and water table depth in peatlands - make
25 a substantial difference to the sensitivities of emissions to environmental drivers, at least over
26 the 12-year period of this study. Even if we do not fully trust the Bousquet2011 inversions, it
27 seems reasonable to assume that the models that simulate high-latitude-specific processes are
28 more likely to be correct in this regard than the other models. These sensitivities have a
29 bearing on models' responses to potential future climate change (e.g., Riley et al., 2011;
30 Koven et al., 2011).

1 Thus, it appears that the following model features are desirable for reliable simulations of
2 boreal wetlands:

- 3 ▪ Realistic soil thermal physics, including freeze-thaw dynamics. Most of the models
4 that were highly correlated with one driver (LPJ-WSL, DLEM, LPJ-MPI, VISIT, and
5 SDGVM) lacked this feature.

- 6 ▪ Accurate representations of peat soils. Again, many of the models with high
7 correlations with one driver (LPJ-WSL, DLEM, VISIT, and SDGVM) lacked this
8 feature.

- 9 ▪ Realistic representations of unsaturated (non-inundated) peatlands, including the
10 dependence of CH₄ emissions on water table depth. LPJ-WSL, an F_w-dominated
11 model, effectively set non-inundated CH₄ emissions to zero because it did not simulate
12 wetlands outside of the time-varying GIEMS surface water area. At the other
13 extreme, IAP-RAS, a T_{air}-dominated model, treated all wetlands in their static map as
14 if they were saturated, thereby eliminating the contribution of soil moisture variability.
15 The relative insensitivity of LPX-BERN's emissions to water table position similarly
16 reduced the contribution of soil moisture variability, although there are too few
17 observations to say whether this is unreasonable.

18 Other model features either made relatively little difference in this study or were severely
19 underrepresented, but warrant further investigation. This is especially true of biogeochemical
20 processes. For example, whether models contained dynamic vegetation (phenology and/or
21 community composition) or dynamic peatland (peat accumulation and loss) components did
22 not affect performance. However, our 12-year study period was likely too short to see the
23 effects of these features. Changes in vegetation community composition may become more
24 important in end-of-century projections (e.g., Alo and Wang, 2008; Kaplan and New, 2006).
25 In particular, recent studies (Koven et al., 2011; Ringeval et al., 2011; Riley et al., 2011) have
26 found a “wetland feedback”, in which vegetation growth in response to future climate change
27 can lower water tables and reduce inundated extents via increased evapotranspiration. This
28 drying effect reduces end-of-century CH₄ emissions from an approximate doubling of current
29 rates without the feedback to only a 20-30% increase with the feedback. Similarly,
30 hydrologic and chemical changes in peat soils, in response to disturbances such as permafrost

1 thaw or drainage for mining or agricultural purposes, may be important in end-of-century
2 projections (e.g., Strack et al., 2004). However, to properly assess the accuracy of dynamic
3 vegetation or peatland schemes and their effects on CH₄ emissions, a longer historical study
4 period, along with longer observational records (including observations of species
5 compositions and soil carbon densities), would be necessary.

6 Other features may warrant further study. Replacing the Cao (1996) model with the model of
7 Walter and Heimann (2000) modestly lowered VISIT's otherwise extreme correlation with
8 T_{air}. It is not clear if this is an inherent difference between the two formulations or just an
9 artifact of their parameter values in VISIT, but it might imply that the Walter and Heimann
10 model is more appropriate for applications at high latitudes. Similarly, nitrogen-carbon
11 interaction had a substantial latitude-dependent effect on mean CH₄ emissions for LPX-
12 BERN (Table 6). Again, the size of the effect could be model-dependent, and potential
13 impacts on sensitivities to climate change might become more apparent over a longer analysis
14 period.

15 Some of the scatter in model sensitivities to drivers may come from differences in the values
16 of parameters related to methane production, methane oxidation, and plant-aided transport,
17 which recent studies (Riley et al., 2011; Berrittella and van Huissteden, 2011) have found to
18 be particularly influential over wetland CH₄ emissions. Investigation of these parameters
19 over the WSL in a model intercomparison can be difficult due to the many large differences
20 among model formulations. As shown in Sections 3.3 and 3.4.2, the methods of
21 biogeochemical parameter selection had far less influence over the model results than the
22 presence or absence of major features such as sophisticated soil thermal physics. Such a
23 comparison would require examination of a subset of the models that have sufficiently similar
24 snow, soil, and water table formulations in order to isolate the effects of microbial and
25 vegetative parameters.

26 Other features that were not investigated here could have potentially large impacts on the
27 response of high-latitude wetlands to future climate change. One such feature is
28 acclimatization, in which soil microbial communities gradually adapt to the long-term mean
29 soil temperature. This feature has been explored in the ORCHIDEE model (Koven et al.,
30 2011; Ringeval et al., 2010), where it greatly reduced the response of wetland CH₄ emissions
31 to long-term temperature changes. Unfortunately, the version of ORCHIDEE used in this

1 study and in the original WETCHIMP study (Melton et al., 2013; Wania et al., 2013) did not
2 use acclimatization. Acclimatization likely would lower ORCHIDEE's correlation with T_{air}
3 over time scales long enough for changes in the long-term mean to be as large as interannual
4 anomalies. Another feature explored by Koven et al. (2011) is the liberation of ancient labile
5 carbon stored in permafrost. As with dynamic vegetation, a robust evaluation of these effects
6 would require a much longer study period.

7 **4.3 Future Needs for Observations and Inversions**

8 The wide disagreement among estimates from observations and inversions hampers our
9 ability to assess model performance. Given the large influence that wetland maps can have on
10 emissions estimates (not only in the WSL, but over larger areas, as shown by Petrescu et al.,
11 2010), care must be taken to select appropriate maps. Ideally, global satellite or map products
12 such as the GLWD (which omitted the northernmost wetlands in the WSL) should be
13 validated against more intensively ground-truthed regional maps such as Sheng2004 and
14 Peregon2008 where such maps exist. Similarly, resolving the discrepancies between the
15 GIEMS and SWAMPS remote sensing surface water products would require verification
16 against independent observations.

17 The large discrepancy between the spatial distributions of emissions from Glagolev2011 and
18 Kim2011 (concentrated in the South) and Winderlich2012 and Bousquet2011K (concentrated
19 in the North) may be due to several reasons. First, the inversions' posterior estimates reflect
20 their prior distributions: Kim2011 used an earlier version of Glagolev2011 (Glagolev et al.,
21 2010) as its prior, while Winderlich2012 and Bousquet2011K both used the Kaplan (2002)
22 distribution as their prior. Second, different types and locations of observations were used:
23 Glagolev2011 was based on in situ chamber measurements of CH_4 fluxes, 80% of which were
24 obtained south of the Ob' River; while Winderlich2012 was based on atmospheric CH_4
25 concentrations observed at towers near or north of the Ob' River. Third, observations were
26 not taken from the same years. Finally, the Winderlich2012 wetland CH_4 emissions may have
27 been influenced by assumed emission rates from fossil fuel extraction and biomass burning,
28 which were not adjusted during the inversion. Efforts like the revision of Glagolev2011 will
29 certainly help in resolving some discrepancies, but all estimates would benefit from
30 incorporating observations over long time periods and wider areas to reduce uncertainties in
31 their long-term means.

1 The global inversions were also subject to uncertainties. For example, while the
2 Bousquet2011 inversions imply that wetland CH₄ emissions in the WSL are not strongly
3 correlated with either F_w or air temperature, the Bousquet2011 inversions' temporal behaviors
4 must be evaluated with caution. The reference inversion's coefficient of variability (CV),
5 which resulted in net negative annual emissions over the WSL in 2004, was substantially
6 higher than the highest model CV. Bousquet et al (2006) noted that their inversions were
7 more sensitive to the interannual variability of wetland emissions than to their mean;
8 accordingly, it is possible that the Bousquet2011 inversions underestimated the long-term
9 mean, thereby raising the CV. Another possibility is that the monthly coefficients that
10 optimized total emissions over all of boreal Asia were not optimal over the WSL alone, since
11 the environmental drivers interacting with wetlands elsewhere may not have been in phase
12 with those in the WSL. A further possibility, given credence by the reference inversion's
13 consistent net negative emissions over all of Boreal Asia in May and June, is that errors in
14 other components of the inversion (e.g., atmospheric OH concentrations, methane oxidation
15 rates, background methane concentrations advected from elsewhere) influenced wetland
16 emissions. Finally, other methane sources that were not accounted for in the inversion might
17 have been attributed to wetlands; for example: geological CH₄ seeps (Etiope et al., 2008),
18 leaks from gas pipelines (Ulmishek, 2003), or lakes (Walter et al., 2006).

19 At the other extreme, the Bloom2010 product exhibited almost no spatial or temporal
20 variability. This might be an artifact of using GRACE data as a proxy for wetland inundation
21 and water table levels. The spatio-temporal accuracy of Bloom2010 must also be questioned,
22 given that it did not use an atmospheric transport model or account for methane oxidation in
23 the atmosphere. Thus, while Bloom2010 provided a useful estimate of long-term mean
24 emissions, it was less helpful in constraining model responses to climate drivers.

25 Another general limitation of inversions and observations, distinct from estimates of long-
26 term mean emissions, is the lack of sufficiently long periods of record to assess model
27 sensitivities to environmental drivers and climate change. The Bousquet2011 inversions and
28 the SWAMPS surface water product are long enough to begin to address this issue at the
29 global scale, but the Bousquet2011 inversions are not optimized for the WSL. Regional
30 inversions such as Kim2011 and Winderlich2012, which might offer more spatially accurate
31 estimates for the WSL than the Bousquet2011 inversions, only offer a single year of posterior
32 emissions. Long records of in situ observations of CH₄ emissions, and the factors that most

1 directly influence these emissions (e.g., soil temperature and water table depth) only exist in a
2 handful of locations (e.g., the Plotnikovo/Bakchar Bog in the WSL; Panikov and Dedysh,
3 2000; Friberg et al., 2003; Glagolev et al., 2011). Indeed, the paucity of long in situ records
4 limited our ability to evaluate LPX-BERN's relatively low sensitivity to water table depth.
5 Year-round observations would also be helpful, as winter emissions are sparsely sampled
6 (Rinne et al., 2007; Kim et al., 2007; Panikov and Dedysh, 2000) and inversions disagree as
7 to the magnitude of winter emissions (Figure 8). The recent implementation of tower
8 networks in the WSL (Sasakawa et al., 2010; Winderlich et al., 2010) show some promise in
9 this regard, as their observations are both multi-year and year-round. More comprehensive
10 observations of emissions from non-wetland methane sources such as seeps, pipe leaks, and
11 lakes, most of which have so far not been accounted for in inversions (although pipe leaks are
12 now being considered; Berchet et al., 2014), would be beneficial in increasing the accuracy of
13 inversions.

14

15 **5 Conclusion**

16 We compared CH₄ emissions from 21 large-scale wetland models, including the models from
17 the WETCHIMP project, to 5 inversions and several observational datasets of CH₄ emissions,
18 surface water area, and total CH₄-producing area over the West Siberian Lowland (WSL),
19 over the period 1993-2004. Despite the large scatter of individual estimates, mean estimates
20 of annual total emissions over the WSL from forward models (5.34 ± 0.54 Tg CH₄ y⁻¹),
21 inversions (6.06 ± 1.22 Tg CH₄ y⁻¹), and observations (3.91 ± 1.29 Tg CH₄ y⁻¹) largely agreed.
22 However, it was clear that reliance on satellite surface water products alone to delineate
23 wetlands caused substantial biases in long-term mean CH₄ emissions over the region. Models
24 and inversions largely agreed on the timing of the seasonal cycle of emissions over the WSL,
25 but some outliers in the timing of peaks in simulated inundated area indicated potential
26 inaccuracies in simulating the timing of snow melt and drainage rates. Models and inversions
27 also displayed a wide range of interannual variability: the CV of the Bousquet2011 reference
28 inversion was more than twice the CVs of all but one model, while the CV of the Bloom2010
29 inversion was essentially zero. Summer CH₄ emissions from the Bousquet2011 inversions
30 exhibited only weak correlations with summer air temperature or inundation. Models that
31 accounted for soil thermal physics and realistic methane-soil moisture relationships similarly
32 tended to have low to moderate correlations with both inundation and air temperature, due in

1 part to the competing influences of temperature and moisture, and in part to the insulating
2 effects of snow and peat soils. In contrast, models lacking these formulations tended to be
3 either inundation- or temperature-dominated (either inundation or temperature accounted for
4 more than 50% of the variance).

5 Based on our findings, we have the following recommendations for simulating CH₄ emissions
6 from high-latitude wetlands:

- 7 • Forward and inverse models should use the best available wetland maps, either as
8 inputs or as targets for optimization of dynamic wetland schemes. Satellite-derived
9 surface water products are a poor proxy for wetland extent, due to a) misclassifying
10 large areas of high-latitude peatlands that can emit methane when the water table is
11 below the surface; b) often including permanent water bodies, whose carbon cycling
12 dynamics can be substantially different from those of wetlands; and c) difficulties in
13 detecting inundation under forest canopies. To improve the accuracy of global
14 wetland map products may require combining information from satellite products and
15 canonical maps.
- 16 • Models must account for emissions from non-inundated wetlands, with realistic
17 relationships between emissions and water table depth.
- 18 • Models should implement realistic soil thermal physics and snow schemes, and
19 account for the presence of peat soils at high latitudes.
- 20 • Multi-year and multi-decade observational and inversion products are crucial for
21 assessing whether model simulations capture the correct sensitivities of wetland CH₄
22 emissions to environmental drivers.

23

24 **Author Contributions**

25 T. J. Bohn and J. R. Melton jointly conceived and designed this study with input from J. O.
26 Kaplan. J. R. Melton provided the results from the original WETCHIMP models. T. J. Bohn,
27 A. Ito, T. Kleinen, R. Spahni, B. D. Stocker, B. Zhang, and X. Zhu provided results for the
28 other non-WETCHIMP models. R. Schroeder and K. C. McDonald provided the SWAMPS
29 dataset. M. V. Glagolev provided the Glagolev et al. (2011) dataset and information on fossil
30 methane seeps. S. Maksyutov provided the Kim et al. (2011) inversion and the Peregón et al.

1 (2008) wetland map. V. Brovkin provided the Winderlich (2012) inversion. T. J. Bohn
2 processed and reformatted results of all models, observations, and inversions; and analyzed
3 the results. T. J. Bohn and J. R. Melton collaborated on all figures. T. J. Bohn prepared the
4 manuscript with contributions from all co-authors.

5

6 **Acknowledgements**

7 The WETCHIMP project received support for collaboration from the COST Action
8 TERRABITES (ES0804). We thank Dr. Dennis P. Lettenmaier at the University of
9 Washington and NASA grant NNX11AR16G from the Northern Eurasian Earth Science
10 Partnership Initiative (NEESPI) for the use of computational resources. T. J. Bohn was
11 supported by grant 1216037 from the U.S. National Science Foundation (NSF) Science,
12 Engineering and Education for Sustainability (SEES) Post-Doctoral Fellowship program. J.
13 R. Melton was supported by a National Science and Engineering Research Council of Canada
14 (NSERC) visiting Post-Doctoral Fellowship. T. Kleinen was supported by the German
15 Ministry of Education and Research (CarboPerm-Project, BMBF Grant No. 03G0836C). R.
16 Spahni was supported by the Swiss National Science Foundation and by the European
17 Commission through the FP7 project Past4Future (grant No. 243908). B. D. Stocker was
18 supported by ERC FP7 project EMBRACE (grant No. 282672). H. Tian and B. Zhang were
19 supported by US National Science Foundation (EaSM: AGS-1243220). Q. Zhuang and X.
20 Zhu were supported by the US Department of Energy with project No. DE-SC0007007. M.
21 V. Glagolev was supported by a grant in accordance with the Tomsk State University
22 Competitiveness Improvement Program. S. Maksyutov was supported by Grant A-1202 of
23 Environment Research and Technology Development Fund (ERTDF), Ministry of
24 Environment Japan. S. N. Denisov and A. V. Eliseev were supported by the Russian
25 President grant NSh-3894.2014.5 and by the Russian Foundation for Basic Research grant 15-
26 05-02457. A. Gallego-Sala was supported by a Natural Environment Research Council grant
27 (NERC Standard grant NE/I012915/1). W. J. Riley and Z. M. Subin were supported by the
28 US Department of Energy contract No. DE-AC02-05CH11231 under the Regional and Global
29 Climate Modeling (RGCM) Program and the Next-Generation Ecosystem Experiments
30 (NGEE Arctic) project. We thank Dr. Ben Poulter, at Montana State University, and Dr. Elke
31 Hodson, at the U.S. Department of Energy, for the results of LPJ-WSL. We thank Dr. Rita
32 Wania for the results of LPJ-WhyMe. We thank Dr. Bruno Ringeval, at the Institut National

1 de la Recherche Agronomique, France, for the results of ORCHIDEE. We thank Dr. Peter
2 Hopcroft and Dr. Joy Singarayer, at University of Bristol, U.K., for the results of SDGVM.
3 We thank Dr. A. Anthony Bloom, at the University of Edinburgh, U.K., for the Bloom et al.
4 (2010) inversion. We thank Dr. Philippe Bousquet, at the Laboratoire des Sciences du Climat
5 et de l'Environnement, France, for the Reference and Kaplan inversions from Bousquet et al.
6 (2011). We thank Dr. Catherine Prigent, at the Observatoire de Paris, France, and Dr. Fabrice
7 Papa, at the Laboratoire d'Etudes en Géophysique et Oceanographie Spatiales, France, for the
8 GIEMS dataset. We thank Dr. Laurence Smith at the University of California, Los Angeles,
9 for the Sheng et al. (2004) dataset. We thank Dr. Anna Peregon, at Laboratoire des Sciences
10 du Climat et de l'Environnement, France, for the Peregon et al. (2008) dataset. We thank Dr.
11 Elaine Matthews, at NASA/Goddard Institute for Space Studies, for valuable feedback.
12

1 **References**

- 2 Alo, C. A., and Wang, G.: Potential future changes of the terrestrial ecosystem based on
3 climate projections by eight general circulation models, *J. Geophys. Res.-Biogeo.*, 113(G1),
4 G01004, doi: 10.1029/2007JG000528, 2008.
- 5 Amante, C. and Eakins B. W.: ETOPO1 1 Arc-Minute Global Relief Model: Procedures, Data
6 Sources and Analysis, NOAA Technical Memorandum NESDIS NGDC-24, National
7 Geophysical Data Center, NOAA, doi: 10.7289/V5C8276M [last access: April 2013], 2009.
- 8 Berchet, A., Pison, I., Chevallier, F., Paris, J.-D., Bousquet, P., Bonne, J.-L., Arshinov, M. Y.,
9 Belan, B. D., Cressot, C., Davydov, D. K., Dlugokencky, E. J., Fofonov, A. V., Galanin, A.,
10 Lavric, J., Machida, T., Parker, R., Sasakawa, M., Spahni, R., Stocker, B. D., and Winderlich,
11 J.: Natural and anthropogenic methane fluxes in Eurasia: a meso-scale quantification by
12 generalized atmospheric inversion, *Biogeosciences Discuss.*, 11, 14587-14637, doi:
13 10.5194/bgd-11-14587-2014, 2014.
- 14 Berrittella, C., and van Huissteden, J.: Uncertainties in modeling CH₄ emissions from
15 northern wetlands in glacial climates: the role of vegetation parameters, *Clim. Past*, 7(4),
16 1075-1087, doi: 10.5194/cp-7-1075-2011, 2011.
- 17 Beven, K. J., and Kirkby, M. J.: A physically based, variable contributing area model of basin
18 hydrology, *Hydrol. Sci. Bull.*, 24, 43-69, 1979.
- 19 Bloom, A. A., Palmer, P. I., Fraser, A., Reay, D. S., and Frankenburg, C.: Large-Scale
20 Controls of Methanogenesis Inferred from Methane and Gravity Spaceborne Data, *Science*,
21 327, 322, doi: 10.1126/science.1175176, 2010.
- 22 Bohn, T. J., Lettenmaier, D. P., Sathulur, K., Bowling, L. C., Podest, E., McDonald, K. C.,
23 and Friborg, T.: Methane emissions from western Siberian wetlands: heterogeneity and
24 sensitivity to climate change, *Environ. Res. Lett.*, 2(4), 045015, doi: 10.1088/1748-
25 9326/2/4/045015, 2007.
- 26 Bohn, T. J., Podest, E., Schroeder, R., Pinto, N., McDonald, K. C., Glagolev, M., Filippov, I.,
27 Maksyutov, S., Heimann, M., Chen, X., and Lettenmaier, D. P.: Modeling the large-scale

1 effects of surface moisture heterogeneity on wetland carbon fluxes in the West Siberian
2 Lowland, *Biogeosciences*, 10, 6559-6576, doi: 10.5194/bg-10-6559-2013, 2013.

3 Bousquet, P., Ciais, P., Miller, J. B., Dlugokencky, E. J., Hauglustaine, D. A., Prigent, C.,
4 Van der Werf, G. R., Peylin, P., Brunke, E.-G., Carouge, C., Langenfelds, R. L., Lathière, J.,
5 Papa, F., Ramonet, M., Schmidt, M., Steele, L. P., Tyler, S. C., and White, J.: Contribution of
6 anthropogenic and natural sources to atmospheric methane variability, *Nature*, 443, doi:
7 10.1038/nature05132, 2006.

8 Bousquet, P., Ringeval, B., Pison, I., Dlugokencky, E. J., Brunke, E.-G., Carouge, C.,
9 Chevallier, F., Fortems-Cheiney, A., Frankenberg, C., Hauglustaine, D. A., Krummel, P. B.,
10 Langenfelds, R. L., Ramonet, M., Schmidt, M., Steele, L. P., Szopa, S., Yver, C., Viovy, N.,
11 and Ciais, P.: Source attribution of the changes in atmospheric methane for 2006-2008,
12 *Atmos. Chem. Phys.*, 11, 3689-3700, doi: 10.5194/acp-11-3689-2011, 2011.

13 Bovensmann, H., Burrows, J. P., Buchwitz, M., Frerick, J., Noël, S., Rozanov, V. V., Chance,
14 K. V., and Goede, A. P. H.: *SCIAMACHY: Mission objectives and measurement modes*, *J.*
15 *Atmos. Sci.*, 56(2), 127-150, 1999.

16 Brown, J., Ferrians Jr, O. J., Heginbottom, J. A., and Melnikov, E. S.: *Circum-Arctic map of*
17 *permafrost and ground-ice conditions*, Boulder, CO: National Snow and Ice Data
18 Center/World Data Center for Glaciology, Digital media, 1998.

19 Cao, M. K., Marshall, S., and Gregson, K.: Global carbon exchange and methane emissions
20 from natural wetlands: Application of a process-based model, *J. Geophys. Res.-Atmos.*,
21 101(D9), 14399-14414, 1996.

22 Carroll, M.L., Townshend, J. R., DiMiceli, C. M., Noojipady, P., and Sohlberg, R. A.: A new
23 global raster water mask at 250 m resolution, *Int. J. Digital Earth*, 2(4), 291-308, doi:
24 10.1080/17538940902951401, 2009.

25 Christensen, T. R., Ekberg, A., Strom, L., Mastepanov, M., Panikov, N., Öquist, M.,
26 Svensson, B. H., Martikainen, P. J., and Oskarsson, H.: Factors controlling large scale
27 variations in methane emissions from wetlands, *Geophys. Res. Lett.*, 30(7), 1414, doi:
28 10.1029/2002GL016848, 2003.

- 1 Christensen, T. R., Johansson, R. T., Akerman, H. J., Mastepanov, M., Malmer, N., Friborg,
2 T., Crill, P., and Svensson, B. H.: Thawing sub-arctic permafrost: Effects on vegetation and
3 methane emissions, *Geophys. Res. Lett.*, 31(4), L04501, doi: 10.1029/2003GL018680, 2004.
- 4 Clymo, R. S., Kramer, J. R., and Hammerton, D.: Sphagnum-dominated peat bog: a naturally
5 acid ecosystem [and discussion], *Philos. T. R. Soc. Lond.*, B305, 487-499, doi:
6 10.1098/rstb.1984.0072, 1984.
- 7 Dorrepaal, E., Toet, S., van Logtestijn, R. S., Swart, E., van de Weg, M. J., Callaghan, T.V.,
8 and Aerts, R.: Carbon respiration from subsurface peat accelerated by climate warming in the
9 subarctic, *Nature*, 460(7255), 616-619, doi: 10.1038/nature08216, 2009.
- 10 Efremova, T. T., Sekretenko, O. P., Avrova, A. F., and Efremov, S. P.: Spatial structure of
11 acid properties of litter in the succession row of swamp birch woods, *Biol. Bull.*, 41(3), doi:
12 10.1134/S106235901305004X, 2014.
- 13 Eliseev, A. V., Mokhov, I. I., Arzhanov, M. M., Demchenko, P. F., and Denisov, S. N.:
14 Interaction of the methane cycle and processes in wetland ecosystems in a climate model of
15 intermediate complexity, *Izv. Atmos. Ocean. Phy.*, 44(2), 139-152, doi:
16 10.1134/S0001433808020011, 2008.
- 17 Eppinga, M. B., Rietkerk, M., Borren, W., Lapshina, E. D., Bleuten, W., and Wassen, M. J.:
18 Regular surface patterning of peatlands: Confronting theory with field data, *Ecosystems*,
19 11(4), 520-536, doi: 10.1007/s10021-008-9138-z, 2008.
- 20 Etiope, G., Lassey, K. R., Klusman, R. W., and Boschi, E.: Reappraisal of the fossil methane
21 budget and related emission from geologic sources, *Geophys. Res. Lett.*, 35, L09307, doi:
22 10.1029/2008GL033623, 2008.
- 23 ETOPO: 2-minute gridded global relief data (ETOPO2v2), US Department of Commerce,
24 National Oceanic and Atmospheric Administration, National Geophysical Data Center,
25 available at: <http://www.ngdc.noaa.gov/mgg/fliers/06mgg01.html> (last access: 14 August
26 2012), 2006.

1 Farr, T. G., Rosen, P. A., Caro, E., Crippen, R., Duren, R., Hensley, S., Kobrick, M., Paller,
2 M., Rogriguez, E., Roth, L., Seal, D., Shaffer, S., Shimada, J., Umland, J., Werner, M., Oskin,
3 M., Burbank, D., and Alsdorf, D.: The shuttle radar topography mission, *Rev. Geophys.*, 45,
4 RG2004, doi: 10.1029/2005RG000183, 2007.

5 Friborg, T., Soegaard, H., Christensen, T. R., and Panikov, N. S.: Siberian wetlands: Where a
6 sink is a source, *Geophys. Res. Lett.*, 30(21), 2129, doi: 10.1029/2003GL017797, 2003.

7 Fridland, V. M.: *Pochvennaya karta RSFSR (Soil map of the RSFSR)*, scale 1:2,500,000, V.
8 V. Dokuchayev Soils Inst., Admin. for Geod. and Cartogr., Gosagroprom, Moscow, 1988.

9 Friedl, M. A., Sulla-Menashe, D., Tan, B., Schneider, A., Ramankutty, N., Sibley, A., and
10 Huang, X.: MODIS Collection 5 global land cover: Algorithm refinements and
11 characterization of new datasets, *Remote Sens. Environ.*, 114(1), 168-182, doi:
12 10.1016/j.rse.2009.08.016, 2010.

13 Frohling, S., Roulet, N., and Lawrence, D.: Issues related to incorporating northern peatlands
14 in to global climate models, *Carbon Cycling in Northern Peatlands*, [Baird, A. J., Belyea, L.
15 R., Comas, X., Reeve, A. S., and Slater, L. D. (Eds.)], 19-35, doi: 10.1029/2008GM000809,
16 2009.

17 Frohling, S., Talbot, J., Jones, M. C., Treat, C. C., Kauffman, J. B., Tuittila, E. S., and Roulet,
18 N.: Peatlands in the Earth's 21st century climate system, *Environ. Rev.*, 19(NA), 371-396,
19 2011.

20 Fung, I., John, J., Lerner, J., Matthews, E., Prather, M., Steele, L. P., and Fraser, P. J.: Three-
21 dimensional model synthesis of the global methane cycle, *J. Geophys. Res.-Atmos.*, 96(D7),
22 13,033-13,065, doi: 10.1029/91JD01247, 1991.

23 Gedney, N., Cox, P. M., and Huntingford, C.: Climate feedback from wetland methane
24 emissions, *Geophys. Res. Lett.*, **31**, L20503, doi: 10.1029/2004GL020919, 2004.

25 Glagolev, M. V., Kleptsova, I. E., Filippov, I. V., Kazantsev, V. S., Machida, T., and
26 Maksyutov, Sh. Sh.: Methane emissions from subtaiga mires of Western Siberia: The

- 1 “standard model” Bc5, Moscow University Soil Science Bulletin, 65(2), 86-93, doi:
2 10.3103/S0147687410020067, 2010.
- 3 Glagolev, M., Kleptsova, I., Filippov, I., Maksyutov, S., and Machida, T.: Regional methane
4 emission from West Siberia mire landscapes, Environ. Res. Lett., 6(4), 045214, doi:
5 10.1088/1748-9326/6/4/045214, 2011.
- 6 Glagolev, M. V., Sabrekov, A. F., Kleptsova, I. E., Filippov, I. V., Lapshina, E. D., Machida,
7 T., and Maksyutov, Sh. Sh.: Methane Emission from Bogs in the Subtaiga of Western Siberia:
8 The Development of Standard Model, Eurasian Soil Science, 45(10), 947-957, doi:
9 10.1134/S106422931210002X, 2012.
- 10 Glagolev, M. V., Filippov, I. V., Kleptsova, I. E., Maksyutov, S. S.: Mathematical modeling
11 in ecology / Proceedings of Third National Conference with International Participation (21-25
12 Oct 2013, Puschino, Russia), Puschino: Institute of Physical, Chemical and Biological
13 Problems of Soils Science RAS., p75-76., In Russian, 2013.
- 14 Gorham, E.: Northern peatlands: role in the carbon cycle and probable responses to climate
15 warming, Ecol. Appl., 1, 182-195, 1991.
- 16 Hodson, E. L., Poulter, B., Zimmermann, N. E., Prigent, C., and Kaplan, J. O.: The El Niño-
17 Southern Oscillation and wetland methane interannual variability, Geophys. Res. Lett., 38,
18 L08810, doi: 10.1029/2011GL046861, 2011.
- 19 Hopcroft, P. O., Valdes, P. J., and Beerling, D. J.: Simulating idealized Dansgaard-Oeschger
20 events and their potential impacts on the global methane cycle, Quaternary Sci. Rev., 30,
21 3258-3268, 2011.
- 22 Hydro1K: HYDRO1K: Website, available at: <https://lta.cr.usgs.gov/HYDRO1K> (last access:
23 1 April 2013), 2013.
- 24 Intergovernmental Panel on Climate Change (IPCC): Climate Change 2013: The Physical
25 Science Basis. Contribution of Working Group I to the Fifth Assessment Report of the
26 Intergovernmental Panel on Climate Change, [Stocker, T.F., D. Qin, G.-K. Plattner, M.
27 Tignor, S.K. Allen, J. Boschung, A. Nauels, Y. Xia, V. Bex and Midgley, P. M. (eds.)].

1 Cambridge University Press, Cambridge, United Kingdom and New York, NY, USA, 1535
2 pp, doi:10.1017/CBO9781107415324, 2013.

3 Ito, A., and Inatomi, M.: Use of a process-based model for assessing the methane budgets of
4 global terrestrial ecosystems and evaluation of uncertainty, *Biogeosciences*, 9, 759-773, doi:
5 10.5194/bg-9-759-2012, 2012.

6 Kalnay, E., Kanamitsu, M., Kistler, R., Collins, W., Deaven, D., Gandin, L., Iredell, M., Saha,
7 S., White, G., Woollen, J., Zhu, Y., Leetmaa, A., Reynolds, R., Chelliah, M., Ebisuzaki, W.,
8 Higgins, W., Janowiak, J., Mo, K. C., Ropelewski, C., Wang, J., Jenne, R., and Joseph, D.:
9 The NCEP/NCAR 40-year reanalysis project, *B. Am. Meteorol. Soc.*, 77, 437-471, doi:
10 10.1175/1520-0477/(1996)077<0477:TNYRP>2.0.CO;2, 1996.

11 Kaplan, J. O.: Wetlands at the Last Glacial Maximum: Distribution and methane emissions,
12 *Geophys. Res. Lett.*, 29(6), 1079, doi: 10.1029/2001GL013366, 2002.

13 Kaplan, J. O., and New, M.: Arctic climate change with a 2 degrees C global warming:
14 Timing, climate patterns and vegetation change, *Climatic Change*, 79(3-4), 213-241, doi:
15 10.1007/s10584-006-9113-7, 2006.

16 Kim, H.-K., Maksyutov, S., Glagolev, M. V., Machida, T., Patra, P. K., Sudo, K., and Inoue,
17 G.: Evaluation of methane emissions from West Siberian wetlands based on inverse
18 modeling, *Environ. Res. Lett.*, 6(3), 035201, doi: 10.1088/1748-9326/6/3/035201, 2011.

19 Kim, Y., Ueyama, M., Nakagawa, F., Tsunogai, U., Harazono, Y., and Tanaka, N.:
20 Assessment of winter fluxes of CO₂ and CH₄ in boreal forest soils of central Alaska estimated
21 by the profile method and the chamber method: a diagnosis of methane emission and
22 implications for the regional carbon budget, *Tellus B*, 59, 223-233, doi: 10.1111/j.1600-
23 0889.2006.00233.x, 2007.

24 Kleinen, T., Brovkin, V., and Schuldt, R. J.: A dynamic model of wetland extent and peat
25 accumulation: results for the Holocene, *Biogeosciences*, 9, 235-248, doi: 10.5194/bg-9-235-
26 2012, 2012.

- 1 Koven, C. D., Ringeval, B., Friedlingstein, P., Ciais, P., Cadule, P., Khvorostyanov, D.,
2 Krinner, G., and Tarnocai, C.: Permafrost carbon-climate feedbacks accelerate global
3 warming, *P. Natl. Acad. Sci. USA*, 108(36), 14769-14774, doi: 10.1073/pnas.1103910108,
4 2011.
- 5 Kremenetski, K. V., Velichko, A. A., Borisova, O. K., MacDonald, G. M., Smith, L. C., Frey,
6 K. E., and Orlova, L. A.: Peatlands of the Western Siberian lowlands: current knowledge on
7 zonation, carbon content and late Quaternary history, *Quaternary Sci. Rev.*, 22, 703-723, doi:
8 10.1016/S0277-3791(02)00196-8, 2003.
- 9 Lawrence, D. M., and Slater, A. G.: Incorporating organic soil into a global climate model,
10 *Clim. Dynam.*, 30(2-3), 145-160, doi: 10.1007/s00382-007-0278-1, 2008.
- 11 Lawrence, D. M., and Slater, A. G.: The contribution of snow condition trends to future
12 ground climate, *Clim. Dynam.*, 34(7-8), 969-981, doi:10.1007/s00382-009-0537-4, 2010.
- 13 Lehner, B., and Döll, P.: Development and validation of a global database of lakes, reservoirs,
14 and wetlands, *J. Hydrol.*, 296(1-4), 1-22, doi: 10.1016/j.jhydrol.2004.03.028, 2004.
- 15 Liang, X., Lettenmaier, D. P., Wood, E. F., and Burges, S. J.: A simple hydrologically based
16 model of land surface water and energy fluxes for GSMs, *J. Geophys. Res.-Atmos.*, 99(D7),
17 14415-14428, 1994.
- 18 Liu, M., Tian, H., Yang, Q., Yang, J., Song, X., Lohrenz, S. E., and Cai, W.: Long-term
19 trends in evapotranspiration and runoff over the drainage basins of the Gulf of Mexico during
20 1901-2008. *Water Resour. Res.*, 49, 1988–2012, doi:10.1002/wrcr.20180, 2013.
- 21 Lupascu, M., Wadham, J. L., Hornibrook, E. R. C., and Pancost, R. D.: Temperature
22 sensitivity of methane production in the permafrost active layer at Stordalen, Sweden: a
23 comparison with non-permafrost northern wetlands, *Arct. Antarct. Alp. Res.*, 44(4), 469-482,
24 doi: 10.1657/1938-4246-44.4.469, 2012.
- 25 Maksyutov, S., Patra, P.K., Onishi, R., Saeki, T. and Nakazawa, T. NIES/FRCGC global
26 atmospheric tracer transport model: description, validation, and surface sources and sinks
27 inversion, *Earth Simulator*, 9, 3-18, 2008.

- 1 Markov, V. S. (Ed.): Karta torfyanykh mestorozhdeniy Zapadno-Sibierskoi ravniny (Map of
2 peat deposits of West Siberian lowland), scale 1:1,000,000, Geol'trofrazvedka, Moscow, 1971.
- 3 Matthews, E., and Fung, I.: Methane emissions from natural wetlands: Global distribution,
4 area, and environmental characteristics of sources, *Global Biogeochem. Cy.*, 1(1), 61-86,
5 1987.
- 6 Matukhin, R. G., and Danilov, V. P. (Eds.): Karta torfyanykh mestorozhdeniy Zapadnoi Sibiri
7 (Map of peat deposits of West Siberia), Ministerstvo Prirodnikh resoursov Rossiiskoi
8 Federatsii, Sibirski NII geologii, Geofiziki I Mineralnogo Syr'ya, scale 1:1,000,000,
9 Geol'trofrazvedka, Moscow, 2000.
- 10 Melton, J. R., Wania, R., Hodson, E., Poulter, B., Ringeval, B., Spahni, R., Bohn, T., Avis, C.
11 A., Beerling, D. J., Chen, G., Eliseev, A. V., Denisov, S. N., Hopcroft, P. O., Lettenmaier, D.
12 P., Riley, W. J., Singarayer, J. S., Subin, Z. M., Tian, H., Zurcher, S., Brovkin, V., van
13 Bodegom, P. M., Kleinen, T., Yu, Z. C., and Kaplan, J. O.: Present state of global wetland
14 extent and wetland methane modelling: Conclusions from a model intercomparison project
15 (WETCHIMP), *Biogeosciences*, 10(2), 753-788, doi:10.5194/bg-10-753-2013, 2013.
- 16 Mitsch, W. J., and J. G. Gosselink: *Wetlands*, Third Edition, John Wiley and Sons, Inc., New
17 York, NY, USA, 2000.
- 18 Mokhov, I. I., Eliseev, A. V., and Denisov, S. N.: Model diagnostics of variations in methane
19 emissions by wetlands in the second half of the 20th century based on reanalysis data,
20 *Doklady Earth Sci.*, 417, 1293–1297, doi:10.1134/S1028334X07080375, 2007.
- 21 Moore, T. R., de Young, A., Bubier, J. L., Humphreys, E. R., Lafleur, P. M., and Roulet, N.
22 T.: A multi-year record of methane flux at the Mer Bleue bog, southern Canada, *Ecosystems*,
23 14, 646-657, doi: 10.1007/s10021-011-9435-9, 2011.
- 24 NASA Land Processes Distributed Active Archive Center (LP DAAC). ASTER L1B.
25 USGS/Earth Resources Observation and Science (EROS) Center, Sioux Falls, South Dakota,
26 2001.
- 27 Naumov, E. M.: Soil map of the north-east of Eurasia, scale 1:2,500,000, V. V. Dokuchaev
28 Soil Inst., Moscow, 1993.

- 1 Pace, M. L., Cole, J. J., Carpenter, S. R., Kitchell, J. F., Hodgson, J. R., Van de Bogert, M. C.,
2 Bade, D. L., Kirtzberg, E. S., and Bastviken, D.: Whole-lake carbon-13 additions reveal
3 terrestrial support of aquatic food webs, *Nature*, 427(6971), 240-243,
4 doi:10.1038/nature02227, 2004.
- 5 Pan, S., Tian, H., Dangal, S. R. S., Zhang, C., Yang, J., Tao, B., Ouyang, Z., Wang, X., Lu,
6 C., Ren, W., Banger, K., Yang, Q., Zhang, B., and Li, X.: Complex spatiotemporal responses
7 of global terrestrial primary production to climate change and increasing atmospheric CO₂ in
8 the 21st century, *PLoS One*, 9(11), e112810, doi:10.1371/journal.pone.0112810, 2014.
- 9 Panikov, N. S., and Dedysh, S. N.: Cold season CH₄ and CO₂ emission from boreal peat bogs
10 (West Siberia): Winter fluxes and thaw activation dynamics, *Global Biogeochem. Cy.*, 14(4),
11 1071-1080, 2000.
- 12 Papa, F., Prigent, C., Aires, F., Jimenez, C., Rossow, W. B., and Matthews, E.: Interannual
13 variability of surface water extent at the global scale, 1993-2004, *J. Geophys. Res.-Atmos.*,
14 115(D12), D12111, doi: 10.1029/2009JD012674, 2010.
- 15 Peregon, A., Maksyutov, S., Kosykh, N. P., Mironycheva-Tokareva, N. P.: Map-based
16 inventory of wetland biomass and net primary production in western Siberia, *J. Geophys.*
17 *Res.-Biogeo.*, 113(G1), doi:10.1029/2007JG000441, 2008.
- 18 Peregon, A., Maksyutov, S., and Yamagata, Y.: An image-based inventory of the spatial
19 structure of West Siberian wetlands, *Environ. Res. Lett.*, 4, 045014, doi: 10.1088/1748-
20 9326/4/4/045014, 2009.
- 21 Petrescu, A. M. R., van Beek, L. P. H., van Huissteden, J., Prigent, C., Sachs, T., Corradi, C.
22 A. R., Parmentier, F. J. W., and Dolman, A. J.: Modeling regional to global CH₄ emissions of
23 boreal and arctic wetlands, *Global Biogeochem. Cy.*, 24(4), BG4009, doi:
24 10.1029/2009GB003610, 2010.
- 25 Prigent, C., Papa, F., Aires, F., Rossow, W. B., and Matthews, E.: Global inundation
26 dynamics inferred from multiple satellite observations, 1993–2000, *J. Geophys. Res.-Atmos.*,
27 112(D12), 305–317, doi: 10.1029/2006JD007847, 2007.

- 1 Repo, M. E., Huttunen, J. T., Naumov, A. V., Chichulin, A. V., Lapshina, E. D., Bleuten, W.,
2 and Martikainen, J. T.: Release of CO₂ and CH₄ from small wetland lakes in western Siberia,
3 *Tellus B*, 59(5), 788-796, doi: 10.1111/j.1600-0889-2007-00301.x, 2007.
- 4 Riley, W. J., Subin, Z. M., Lawrence, D. M., Swenson, S. C., Torn, M. S., Meng, L.,
5 Mahowald, N. M., and Hess, P.: Barriers to predicting changes in global terrestrial methane
6 fluxes: analyses using CLM4Me, and methane biogeochemistry model integrated in CESM,
7 *Biogeosciences*, 8, 1925-1953, doi: 10.5194/gb-8-1925-2011, 2011.
- 8 Ringeval, B., de Noblet-Ducoudré, N., Ciais, P., Bousquet, P., Prigent, C., Papa, F., and
9 Rossow, W. B.: An attempt to quantify the impact of changes in wetland extent on methane
10 emissions on the seasonal and interannual time scales, *Global Biogeochem. Cycles*, 24,
11 GB2003, doi: 10.1029/2008GB003354, 2010.
- 12 Ringeval, B., Friedlingstein, P., Koven, C., Ciais, P., de Noblet-Ducoudré, N., Decharme, B.,
13 and Cadule, P.: Climate-CH₄ feedback from wetlands and its interaction with the climate-CO₂
14 feedback, *Biogeosciences*, 8, 2137-2157, doi: 10.5194/bg-8-2137-2011, 2011.
- 15 Rinne, J., Riutta, T., Pihlatie, M., Aurela, M., Haapanala, S., Tuovinen, J.-P., and Tuittila, E.-
16 S.: Annual cycle of methane emission from a boreal fen measured by the eddy covariance
17 technique, *Tellus B*, 59, 449-457, doi: 10.1111/j.1600-0889.2007.00261.x, 2007.
- 18 Romanova, E. A., Bybina, R. T., Golitsyna, E. F., Ivanova, G. M., Usova, I. I., and
19 Trushnikova, L. G.: Tipologicheskaya karta bolot Zapadno-Sibirskoi ravniny (Typological
20 map of wetlands of West Siberian Lowland), scale 1:2,500,000, GUGK, Moscow, 1977.
- 21 Rödenbeck, C., Gerbig, C., Trusilova, K., and Heimann, M.: A two-step scheme for high-
22 resolution regional atmospheric trace gas inversions based on independent models, *Atmos.*
23 *Chem. Phys.*, 9(14), 5331-5342, doi: 10.5194/acp-9-5331-2009, 2009.
- 24 Saarnio, S., Alm, J., Silvola, J., Lohila, A., Nykänen, H., and Martikainen, P. J.: Seasonal
25 variation in CH₄ emissions and production and oxidation potentials at microsites of an
26 oligotrophic pine fen, *Oecologia*, **110**, 414-422, 1997.

- 1 Sabrekov, A. F., Glagolev, M. V., Kleptsova, I. E., Machida, T., and Maksyutov, S. S.:
2 Methane Emission from Bog Complexes of the West Siberian Taiga, *Eurasian Soil Science*,
3 46 (12), 1182–1193, doi: 10.1134/S1064229314010098, 2013.
- 4 Sabrekov, A. F., Runkle, B. R. K., Glagolev, M. V., Kleptsova, I. E., and Maksyutov, S. S.:
5 Seasonal variability as a source of uncertainty in the West Siberian regional CH₄ flux
6 upscaling, *Environ. Res. Lett.*, 9, 045008, doi: 10.1088/1748-9326/9/4/045008, 2014.
- 7 Sasakawa, M., Shimoyama, K., Machida, T., Tsuda, N., Suto, H., Arshinov, M., Davydov, D.,
8 Fofonov, A., Krasnov, O., Saeki, T., Koyama, Y., and Maksyutov, S.: Continuous
9 measurements of methane from a tower network over Siberia, *Tellus B*, 62(5), 403-416, doi:
10 10.1111/j.1600-0889.2010.00494.x, 2010.
- 11 Sasakawa, M., Ito, A., Machida, T., Tsuda, N., Niwa, Y., Davydov, D., Fofonov, A., and
12 Arshinov, M.: Annual variation of CH₄ emissions from the middle Taiga in West Siberian
13 Lowland (2005-2009): a case of high CH₄ flux and precipitation rate in the summer of 2007,
14 *Tellus B*, 64, 17514, doi: 10.3402/tellusb.v64i0.17514, 2012.
- 15 Schaefer, K., Zhang, T., Bruhwiler, L., and Barrett, A. P.: Amount and timing of permafrost
16 carbon release in response to climate warming, *Tellus B*, 63, 165-180, doi: 10.1111/j.1600-
17 0889.2011.00527.x, 2011.
- 18 Schroeder, R., Rawlins, M. A., McDonald, K. C., Podest, E., Zimmermann, R., and Kueppers,
19 M.: Satellite microwave remote sensing of North Eurasian inundation dynamics: development
20 of coarse-resolution products and comparison with high-resolution synthetic aperture radar
21 data, *Environ. Res. Lett.*, 5(1), 015003, doi: 10.1088/1748-9326/5/1/015003, [available at
22 <http://wetlands.jpl.nasa.gov>], 2010.
- 23 Schuldt, R. J., Brovkin, V., Kleinen, T., and Winderlich, J.: Modelling Holocene carbon
24 accumulation and methane emissions of boreal wetlands – an Earth system model approach,
25 *Biogeosciences*, 10, 1659-1674, doi: 10.5194/bg-10-1659-2013, 2013.
- 26 Schuur, E. A. G., Bockheim, J., Canadell, J. G., Euskirchen, E., Field, C. B., Goryachkin, S.
27 V., Hagemann, S., Kuhry, P., LaFleur, P. M., Lee, H., Mazhitova, G., Nelson, F. E., Rinke,
28 A., Romanovsky, V. E., Shiklomanov, N., Tarnocai, C., Venevsky, S., Vogel, J. G., and

- 1 Zimov, S. A.: Vulnerability of permafrost carbon to climate change: Implications for the
2 global carbon cycle, *Bioscience*, 58(8), 701-714, doi: 10.1641/B580807, 2008.
- 3 Serreze, M. C., Walsh, J. E., Chapin, F. S., Osterkamp, T., Dyurgerov, M., Romanovsky, V.,
4 Oechel, W. C., Morison, J., Zhang, T., and Barry, R. G.: Observational evidence of recent
5 change in the northern high-latitude environment, *Climatic Change*, 46(1-2), 159-207, doi:
6 10.1023/A:1005504031923, 2000.
- 7 Sheng, Y., Smith, L. C., MacDonald, G. M., Kremenetski, K. V., Frey, K. E., Velichko, A.
8 A., Lee, M., Beilman, D. W., and Dubinin, P.: A high-resolution GIS-based inventory of the
9 west Siberian peat carbon pool, *Global Biogeochem. Cy.*, 18(3), GB3004, doi:
10 10.1029/2003GB002190, 2004.
- 11 Shimoyama, K., Hiyama, T., Fukushima, Y., and Inoue, G.: Seasonal and interannual
12 variation in water vapor and heat fluxes in a West Siberian continental bog, *J. Geophys. Res.-*
13 *Atmos.*, 108(D20), 4648, doi: 10.1029/2003JD003485, 2003.
- 14 Sippel, S. J., and Hamilton, S. K.: Determination of inundation area in the Amazon River
15 floodplain using the SMMR 37 GHz polarization difference, *Remote Sens. Environ.*, 76, 70–
16 76, 1994.
- 17 Smith, L. C., Sheng, Y., MacDonald, G. M., and Hinzman, L. D.: Disappearing arctic lakes,
18 *Science*, 308(5727), 1429-1429, doi: 10.1126/science.1108142, 2005.
- 19 Spahni, R., Wania, R., Neef, L., van Weele, M., Pison, I., Bousquet, P., Frankenberg, C.,
20 Foster, P. N., Joos, F., Prentice, I. C., and van Velthoven, P.: Constraining global methane
21 emissions and uptake by ecosystems, *Biogeosciences*, 8, 1643-1665, doi: 10.5194/bg-8-1643-
22 2011, 2011.
- 23 Spahni, R., Joos, F., Stocker, B. D., Steinacher, M., and Yu, Z. C.: Transient simulations of
24 the carbon and nitrogen dynamics in northern peatlands: from the Last Glacial Maximum to
25 the 21st century, *Clim. Past*, 9, 1287-1308, doi:10.5194/cp-9-1287-2013, 2013.

- 1 Stocker, B. D., Roth, R., Joos, F., Spahni, R., Steinacher, M., Zähle, S., Bouwman, L., and
2 Prentice, I. C.: Multiple greenhouse-gas feedbacks from the land biosphere under future
3 climate change scenarios, *Nature Clim. Change*, 3(7), 666-672, 2013.
- 4 Stocker, B. D., Spahni, R., and Joos, F.: DYPTOP: a cost-efficient TOPMODEL
5 implementation to simulate sub-grid spatio-temporal dynamics of global wetlands and
6 peatlands, *Geosci. Model Dev.*, doi: 10.5194/gmd-7-1-2014, 2014.
- 7 Strack, M., Waddington, J. M., and Tuittila, E.-S.: Effect of water table drawdown on
8 northern peatland methane dynamics: Implications for climate change, *Global Biogeochem.*
9 *Cy.*, 18, GB4003, doi: 10.1029/2003GB002209, 2004.
- 10 Subin, Z. M., Milly, P. C., Sulman, B. N., Malyshev, S., and Shevliakova, E.: Resolving
11 terrestrial ecosystem processes along a subgrid topographic gradient for an earth-system
12 model. *Hydrol. Earth Syst. Sci. Discuss.*, 11(7), 8443-8492, doi: 10.5194/hessd-11-8443-
13 2014, 2014.
- 14 Tapley, B. D., Bettadpur, S., Ries, J. C., Thompson, P. F., and Watkins, M. M.: GRACE
15 measurements of mass variability in the Earth system, *Science*, 305(5683), 503-505, doi:
16 10.1126/science.1099192, 2004.
- 17 Tang, J., and Zhuang, Q.: Equifinality in parameterization of process-based biogeochemistry
18 models: A significant uncertainty source to the estimation of regional carbon dynamics, *J.*
19 *Geophys. Res.-Biogeo.*, 113(G4), G04010, doi: 10.1029/2008JG000757, 2008.
- 20 Tarnocai, C., Adams, G. D., Glooschenko, V., Glooschenko, W. A., Grondin, P., Hirvonen,
21 H. E., Lynch-Stewart, P., Mills, G. F., Oswald, E. T., Pollett, F. C., Rubec, C. D. A., Wells, E.
22 D., and Zoltai, S. C., 1988: The Canadian wetland classification system. In *National Wetlands*
23 *Working Group, ed. Wetlands of Canada. Ecological Land Classification Series 24,*
24 *Environment Canada, Ottawa, Ontario, and Polyscience Publications, Montreal, Quebec, pp*
25 *413-427.*
- 26 Tarnocai, C., Canadell, J. G., Schuur, E. A. G., Kuhry, P., Mazhitova, G., and Zimov, S.: Soil
27 organic carbon pools in the northern circumpolar permafrost region, *Global Biogeochem. Cy.*,
28 23, GB2023, doi: 10.1029/2008GB003327, 2009.

- 1 Tian, H., Xu, X., Liu, M., Ren, W., Zhang, C., and Lu, C.: Spatial and temporal patterns of
2 CH₄ and N₂O fluxes in terrestrial ecosystems of North America during 1979-2008:
3 application of a global biogeochemistry model, *Biogeosciences*, 7, 2673-2694, doi:
4 10.5194/bg-7-2673-2010, 2010.
- 5 Tian, H., Melillo, J., Lu, C., Kicklighter, D., Liu, M., Ren, W., Xu, X., Chen, G., Zhang, C.,
6 Pan, S., Liu, J., and Running, S.: China's terrestrial carbon balance: contributions from
7 multiple global change factors, *Global Biogeochem. Cy.*, 25(1), 222-240, doi:
8 10.1029/2010GB003838, 2011a.
- 9 Tian, H., Xu, X., Lu, C., Liu, M., Ren, W., Chen, G., Melillo, J., and Liu, J.: Net exchanges of
10 CO₂, CH₄, and N₂O between China's terrestrial ecosystems and the atmosphere and their
11 contributions of global climate warming, *J. Geophys. Res.-Biogeo.*, 116(G2), G02011, doi:
12 10.1029/2010JG001393, 2011b.
- 13 Tian, H., Lu, G., Chen, G., Tao, S., Pan, S., Del Grosso, S. J., Xu, X., Bruhwiler, L., Wofsy,
14 S. C., Kort, E. A., and Prior, S. A.: Contemporary and projected biogenic fluxes of methane
15 and nitrous oxide in terrestrial ecosystems of North America, *Front. Ecol. Environ.*, 10(10),
16 528-536, doi: 10.1890/120057, 2012.
- 17 Trusilova, K., Rödenbeck, C., Gerbig, C., and Heimann, M.: Technical note: A new coupled
18 system for global-to-regional downscaling of CO₂ concentration estimation, *Atmos. Chem.*
19 *Phy.*, 10(7), 3205-3213, 2010.
- 20 Ulmishek, G. F, *Petroleum geology and resources of the West Siberian Basin, Russia*, US
21 Department of the Interior, US Geological Survey, Washington, DC, 2003.
- 22 Umezawa, T., Machida, T., Aoki, S., and Nakazawa, T.: Contributions of natural and
23 anthropogenic sources to atmospheric methane variations over western Siberia estimated from
24 its carbon and hydrogen isotopes, *Global Biogeochem. Cycles*, 26(4), GB4009, doi:
25 10.1029/2011GB004232, 2012.
- 26 van Huissteden, J., Petrescu, A. M. R., Hendriks, D. M. D., and Rebel, K.T.: Sensitivity
27 analysis of a wetland methane emission model based on temperate and arctic wetland sites,
28 *Biogeosciences*, 6, 3035-3051, doi: 10.5194/bg-6-3035-2009, 2009.

1 Viovy, N. and Ciais, P.: CRUNCEP data set for 1901–2008, Tech. Rep. Version 4,
2 Laboratoire des Sciences du Climat et de l'Environnement, available at:
3 [http://dods.extra.ccea.fr/data/p529viov/cruncep/](http://dods.extra cea.fr/data/p529viov/cruncep/), last access: 1 September 2011.

4 Walter, B. P., and Heimann, M.: A process-based, climate-sensitive model to derive methane
5 emissions from natural wetlands: Application to five wetland sites, sensitivity to model
6 parameters, and climate, *Global Biogeochem. Cy.*, 14(3), 745-765, doi:
7 10.1029/1999GB001204, 2000.

8 Walter, K. M., Zimov, S. A., Chanton, J. P., Verbyla, D., and Chapin, F. S.: Methane
9 bubbling from Siberian thaw lakes as a positive feedback to climate warming, *Nature*,
10 443(7107), 71-75, doi: 10.1038/05040, 2006.

11 Wania, R., Ross, I., and Prentice, I. C.: Integrating peatlands and permafrost into a dynamic
12 global vegetation model: 1. Evaluation and sensitivity of physical land surface processes,
13 *Global Biogeochem. Cy.*, 23(3), GB3014, doi:10.1029/2008GB003412, 2009a.

14 Wania, R., Ross, I., and Prentice, I. C.: Integrating peatlands and permafrost into a dynamic
15 global vegetation model: 2. Evaluation and sensitivity of vegetation and carbon cycle
16 processes, *Global Biogeochem. Cy.*, 23(3), GB3015, doi:10.1029/2008GB003413, 2009b.

17 Wania, R., Ross, I., and Prentice, I. C.: Implementation and evaluation of a new methane
18 model within a dynamic global vegetation model: LPJ-WHyMe v1.3.1, *Geosci. Model. Dev.*,
19 3, 565-584, doi:10.5194/gmd-3-565-2010, 2010.

20 Wania, W., Melton, J. R., Hodson, E. L., Poulter, B., Ringeval, B., Spahni, R., Bohn, T., Avis,
21 C. A., Chen, G., Eliseev, A. V., Hopcroft, P. O., Riley, W. J., Subin, Z. M., Tian, H., van
22 Bodegom, P. M., Kleinen, T., Yu, Z. C., Sinarayer, J. S., Zürcher, S., Lettenmaier, D. P.,
23 Beerling, D. J., Denisov, S. N., Prigent, C., Papa, F., and Kaplan, J. O.: Present state of global
24 wetland extent and wetland methane modelling: methodology of a model inter-comparison
25 project (WETCHIMP), *Geosci. Model Dev.*, 6, 617-641, doi: 10.5194/gmd-6-617-2013, 2013.

26 WETCHIMP-WSL: http://arve.unil.ch/pub/wetchimp/wetchimp_wsl, last access: 21 January,
27 2015.

- 1 Winderlich, J., Chen, H., Gerbig, C., Seifert, T., Kolle, O., Lavrič, J. V., Kaiser, C., Höfer, A.,
2 and Heimann, M.: Continuous low-maintenance CO₂/CH₄/H₂O measurements at the Zotino
3 Tall Tower Observatory (ZOTTO) in Central Siberia, *Atmos. Meas. Tech.*, 3, 1113-1128, doi:
4 10.5194/amt-3-1113-2010, 2010.
- 5 Winderlich, J.: Setup of a CO₂ and CH₄ measurement system in Central Siberia and modeling
6 of its results, Technical Reports 26, Max-Planck-Institut für Biogeochemie, Jena, pp. 120,
7 2012.
- 8 Zhang, T.: Influence of the seasonal snow cover on the ground thermal regime: an overview,
9 *Rev. Geophys.*, 43, RG4002, doi: 10.1029/2004RG000157, 2005.
- 10 Zhu, X., Zhuang, Q., Lu, X., and Song, L.: Spatial scale-dependent land-atmosphere methane
11 exchanges in the northern high latitudes from 1993 to 2004, *Biogeosciences*, 11, 1693-1704,
12 doi: 10.5194/bg-11-1693-2014, 2014.
- 13 Zhuang, Q., Melillo, J. M., Kicklighter, D. W., Prinn, R. G., McGuire, A. D., Steudler, P. A.,
14 Felzer, B. S., and Hu, S.: Methane fluxes between terrestrial ecosystems and the atmosphere
15 at northern high latitudes during the past century: A retrospective analysis with a process-
16 based biogeochemistry model, *Global Biogeochem. Cy.*, 18, GB3010, doi:
17 10.1029/2004GB002239, 2004.
- 18 Zürcher, S., Spahni, R., Joos, F., Steinacher, M., Fischer, H.: Impact of an abrupt cooling
19 event on interglacial methane emissions in northern peatlands, *Biogeosciences*, 10(3), 1963-
20 1981, 2013.
- 21

1 Tables

2 Table 1. Observations and inversions used in this study.

Name	Reference	Description	Temporal Domain	Temporal Resolution	Spatial Domain	Spatial Resolution
Wetland Maps						
Sheng2004	Sheng et al. (2004)	Wetland map of WSL based on digitization of regional maps of Markov (1971), Matukhin and Danilov (2000), and Romanova et al (1977). Supplemented with peat cores.	2 nd half of 20 th Century	Static map	West Siberia	1:2,500,000 north of 65° N, 1:1,000,000 south of 65° N
Peregon2008	Peregon et al. (2008)	Wetland map of WSL based on digitization of regional map of Romanova et al (1977). Wetland types identified by remote sensing and field validation.	2 nd half of 20 th Century	Static map	West Siberia	1:2,500,000
Northern Circumpolar Soil Carbon Database (NCSCD)	Tarnocai et al. (2009)	Map of soil types across the northern circumpolar permafrost region. Over the WSL, based on maps of Fridland (1988) and Naumov (1993).	2 nd half of 20 th Century	Static map	Northern circumpolar permafrost region	1:2,500,000
Global Lake and Wetland Database (GLWD)	Lehner and Döll (2004)	Global lake and wetland map. Wetlands were the union of four global datasets.	2 nd half of 20 th Century	Static map	Global	1:1,000,000
Surface Water						
Global Inundation Extent from Mult-Satellites (GIEMS)	Papa et al. (2010)	Remote sensing surface water product based on visible/near-infrared (AVHRR) and active (SSM/I) and passive (ERS) microwave sensors.	1993-2004	Daily, aggregated to monthly	Global	25km equal area grid, aggregated to 0.5 × 0.5°
Surface Water Microwave Product Series (SWAMPS)	Schroeder et al. (2010)	Remote sensing surface water product based on active (SeaWinds-on-QuikSCAT, ERS, and ASCAT) and passive (SSM/I, SSMI/S) microwave sensors.	1992-2013	Daily, aggregated to monthly	Global	25km equal area grid, aggregated to 0.5 × 0.5°

CH ₄ Inventory						
Glagolev2011	Glagolev et al. (2011)	In situ flux sampling along transect spanning West Siberia, 2006-2010; statistical model of fluxes as function of wetland type applied to map of Peregon et al. (2008).	2006-2010	Monthly climatology	West Siberia	0.5 × 0.5°
CH ₄ Inversions						
Bloom2010	Bloom et al. (2010)	Global optimization of relationship between atmospheric CH ₄ concentrations (Bovensmann et al., 1999), NCEP/NCAR surface temperatures (Kalnay et al., 1996), and GRACE gravity anomalies (Tapley et al., 2004)	2003-2007	Annual	Global	3 × 3°
Bousquet2011R	Bousquet et al. (2011), Bousquet et al. (2006)	Global inversion using LMDZ with Matthews and Fung (1987) inventory as the wetland prior.	1993-2009	Monthly	Global	1×1° resolution for prior, multiplied by single coefficient for all of Boreal Asia
Bousquet2011K	Bousquet et al. (2011), Bousquet et al. (2006)	Global inversion using LMDZ with emissions from Kaplan (2002) as the wetland prior.	1993-2009	Monthly	Global	1×1° resolution for prior, multiplied by single coefficient for all of Boreal Asia
Kim2011	Kim et al. (2011)	Global inversion, with Glagolev et al (2010) as prior in WSL, Fung et al. (1991) elsewhere	2002-2007	Monthly climatology	Regional	1 × 1° resolution for prior, multiplied by single coefficient for all of WSL
Winderlich2012	Winderlich (2012), Schuldt et al. (2013)	Regional inversion over West Siberia, with Kaplan (2002) as the wetland prior	2009	Monthly climatology	Regional	1 × 1° resolution for both prior and coefficients over WSL

1

2 Table 2. Participating models and their relevant hydrologic features.

Model	Reference	Configuration ¹	Period	Observational Constraints on CH ₄ -Producing Areas				Unsaturated Emissions? ⁶	Water Table ⁴	Organic Soil ⁷	Soil Freeze/Thaw ⁸
				Surface Water ²	Topography ³	Maps ⁴	Code ⁵				
CLM4ME	Riley et al. (2011)	CLM4ME	1993-2004	GIEMS	-	-	S ^a	Yes	Uniform	Yes	Yes
DLEM	Tian et al. (2010, 2011a,b, 2012)	DLEM	1993-2004	GIEMS	-	-	S	Yes	Uniform	No	No
DLEM2	Tian et al. (2010, 2011a,b, 2012)	DLEM2	1993-2004	GIEMS	-	-	S	Yes	Uniform	Yes	Yes
IAP-RAS	Mokhov et al. (2007), Eliseev et al. (2008)	IAP-RAS	1993-2004	-	-	CDIAC NDP017 ^b	M,M+	No	n/a	Yes	Yes
LPJ-Bern	Spahni et al. (2011), Zürcher et al. (2013)	LPJ-Bern	1993-2004	GIEMS	-	NCSCD	M	Yes	Uniform	Yes	Yes
LPJ-MPI	Kleinen et al. (2012)	LPJ-MPI	1993-2010	-	Hydro1K ^c	-	T	Yes	TOPMODEL	Yes	No

LPJ-WHyMe	Wania et al. (2009a,b; 2010)	LPJ-WHyMe	1993-2004	-	-	NCSCD	M	Yes	Microtopography	Yes	Yes
LPJ-WSL	Hodson et al. (2011)	LPJ-WSL	1993-2004	GIEMS	-	-	S	No	n/a	No	No
LPX-BERN	Spahni et al. (2013), Stocker et al. (2013),	LPX-BERN	1993-2010	GIEMS for inundated non-peatland wetlands	-	Peregon2008 for peatland fraction	M,M+	Yes	Uniform	Yes	Yes
	Stocker et al. (2014)	LPX-BERN (DYPTOP)	1993-2010	-	ETOPO1 ^d , Hydro1K ^c	-	T	Yes	TOPMODEL	Yes	Yes
		LPX-BERN (N)	1993-2010	GIEMS for inundated non-peatland wetlands	-	Peregon2008 for peatland fraction	M,M+	Yes	Uniform	Yes	Yes
		LPX-BERN (DYPTOP-N)	1993-2010	-	ETOPO1 ^d , Hydro1K ^c	-	T	Yes	TOPMODEL	Yes	Yes
ORCHIDEE	Ringeval et al. (2010)	ORCHIDEE	1993-2004	GIEMS	Hydro1K ^c	-	S ^a	Yes	TOPMODEL	Yes	Yes
SDGVM	Hopcroft et al. (2011)	SDGVM	1993-2004	-	ETOPO 2v2 ^e	-	T	Yes	Uniform	No	No
UW-VIC	Bohn et al. (2013)	UW-VIC (GIEMS)	1993-2004	GIEMS	SRTM ^f , ASTER ^g	Sheng2004	M,M+	Yes	Microtopography	Yes	Yes
		UW-VIC (SWAMPS)	1993-2010	SWAMPS	SRTM ^f , ASTER ^g	Sheng2004	M,M+	Yes	Microtopography	Yes	Yes

VIC-TEM- TOPMODEL	Zhu et al. (2014)	VIC-TEM- TOPMODEL	1993-2004	GIEMS	Hydro1K ^c		T	Yes	TOPMODEL	No	Yes
VISIT	Ito and Inatomi (2012)	VISIT (GLWD)	1993-2010	-	-	GLWD	M,M+	Yes	Uniform	No	No
		VISIT (SHENG)	1993-2010	-	-	Sheng2004	M,M+	Yes	Uniform	No	No
		VISIT (GLWD- WH)	1993-2010	-	-	GLWD	M,M+	Yes	Uniform	No	No
		VISIT (SHENG- WH)	1993-2010	-	-	Sheng2004	M,M+	Yes	Uniform	No	No

1

2 ¹Configuration: Short name identifying both the model and the parameter/feature settings for a particular simulation; for models that
3 contributed only a single simulation, the configuration equals the model name

4 ²Surface Water: Name of time-varying surface water product (if any) used as a constraint on CH₄-contributing area

5 ³Topography: Name of topographic product (if any) used as a constraint on CH₄-contributing area

6 ⁴Map: Name of static wetland map product (if any) used as a constraint on CH₄-contributing area

7 ⁵Code: Single-letter code summarizing the types of CH₄-contributing area constraints used (“S” = surface water only; “T” = topography with
8 or without surface water constraint; “M” = static wetland map with or without surface water or topography constraints; “M+” = subset of M
9 that excludes the NCSCD)

1 ⁶Water Table: approach used to account for water table depths (“uniform” = water table depth is the same at all wetland points within the grid
 2 cell; “TOPMODEL” = water table depth varies spatially within the grid cell as a function of topography, following a TOPMODEL approach
 3 (Beven and Kirkby, 1979); “microtopography” = water table depth varies spatially within the grid cell as a function of assumed
 4 microtopography; “n/a” = not applicable)

5 ⁷Soil Freeze/Thaw: “Yes” or “No” indicates whether the model accounts for the freezing and thawing of water within the soil column

6 ^aCLM4Me and ORCHIDEE are listed as “S” due to tuning/rescaling of inundated areas to match GIEMS, thus destroying contribution of
 7 topography.

8 ^b<http://cdiac.esd.ornl.gov/ndps/ndp017.html>

9 ^cHydro1K (2013)

10 ^dAmante and Eakins (2009)

11 ^eETOPO (2006)

12 ^fFarr et al. (2007)

13 ^gNASA (2001)

14

15 Table 3. Participating models and their relevant biogeochemical features.

Model	$R_{anaerobic}/R_{aerobic}$ ¹	C Substrate Source ²	pH ³	Redox State ⁴	Dynamic Vegetation ⁵	Nitrogen-Carbon Cycle Interaction ⁶	Saturated NPP Inhibition ⁷	Parameter Selection ⁸
CLM4Me	Variable	Cpool	Yes	Yes	Yes	Yes	No	Optimized to various sites

DLEM	Variable	NPP & Cpool	Yes	Yes	No	No	No	Optimized to various sites
DLEM2	Variable	NPP & Cpool	Yes	Yes	No	No	No	Optimized to various sites
IAP-RAS	n/a	Cpool	No	No	No	No	No	Literature; Scaled to global total
LPJ-Bern	Constant	NPP & Cpool	No	No	Yes	No	Yes	Optimized to various sites; Scaled to global total
LPJ-MPI	Constant	Cpool	No	No	Yes	No	Yes	Literature
LPJ-WHyMe	Constant	NPP & Cpool	No	No	Yes	No	Yes	Literature; Scaled to global total
LPJ-WSL	Constant	Cpool	No	No	Yes	No	No	Literature
LPX-BERN	Constant	NPP & Cpool	No	No	Yes	No	Yes	Optimized to various sites; Scaled to global total
LPX-BERN (DYPTOP)	Constant	NPP & Cpool	No	No	Yes	No	Yes	Optimized to various sites; Scaled to global total
LPX-BERN (N)	Constant	NPP & Cpool	No	No	Yes	Yes	Yes	Optimized to various sites; Scaled to global total
LPX-BERN (DYPTOP-N)	Constant	NPP & Cpool	No	No	Yes	Yes	Yes	Optimized to various sites; Scaled to global total
ORCHIDEE	Variable	Cpool	No	No	Yes	No	No	Literature and Optimized to various sites
SDGVM	Variable	Cpool	No	No	Yes	No	No	Literature
UW-VIC(GIEMS)	Variable	NPP	No	No	No	No	Yes	Optimized to sites in Glagolev2011
UW-VIC(SWAMPS)	Variable	NPP	No	No	No	No	Yes	Optimized to sites in Glagolev2011
VIC-TEM- TOPMODEL	Variable	NPP	Yes	Yes	No	No	No	Optimized to various sites

VISIT(GLWD)	Variable	Cpool	No	No	No	Yes (only affects upland CH ₄ oxidation)	No	Literature
VISIT(GLWD-WH)	Variable	NPP	No	No	No	Yes (only affects upland CH ₄ oxidation)	No	Literature
VISIT(Sheng)	Variable	Cpool	No	No	No	Yes (only affects upland CH ₄ oxidation)	No	Literature
VISIT(Sheng-WH)	Variable	NPP	No	No	No	Yes (only affects upland CH ₄ oxidation)	No	Literature

1 ¹R_{anaerobic}/R_{aerobic}: How the ratio of anaerobic to aerobic respiration is handled in the model (“Constant” = ratio is held constant; “Variable” =
2 ratio varies either as an explicit function of environmental conditions or as the result of separate governing equations for aerobic and
3 anaerobic respiration; “n/a” = not applicable)

4 ²Carbon Substrate Source: “Cpool” = soil carbon pool; “NPP” = root exudates, in proportion to net primary productivity

5 ³pH: indicates whether soil pH influences CH₄ emissions

6 ⁴Redox State: indicates whether soil redox state influences CH₄ emissions

7 ⁵Dynamic Vegetation: indicates whether vegetation species abundances change in response to environmental conditions

8 ⁶Nitrogen-Carbon Cycle Interaction: indicates whether interactions between the nitrogen and carbon cycles influence CH₄ emissions

9 ⁷Saturated NPP Inhibition: indicates whether NPP decreases under wet soil conditions for any plant species

10 ⁸Parameter Selection: method of choosing parameter values (“Literature” = values chosen from ranges reported in literature; “Optimized” =
11 values chosen to minimize the difference between simulated and observed values, either of CH₄ fluxes at selected sites or of global
12 atmospheric CH₄ concentrations)

1

2

3 Table 4. Estimates of June-July-August CH₄ emissions from subsets of the participating models, over the entire WSL and its Southern (< 61°
 4 N) and Northern halves, for the period 1993-2004. Biases were computed with respect to the Glagolev2011/Peregon2008 estimates.

Subset	Average June-July-August CH ₄ (Tg CH ₄ mon ⁻¹)									Average June-July-August CH ₄ -Producing Area (10 ³ km ²)								
	WSL			South			North			WSL			South			North		
	Mean	Bias	Std. Dev.	Mean	Bias	Std. Dev.	Mean	Bias	Std. Dev.	Mean	Bias	Std. Dev.	Mean	Bias	Std. Dev.	Mean	Bias	Std. Dev.
I	1.10	0.14	0.37	0.22	-0.45	0.16	0.89	0.59	0.24	388	-291	136	66	-270	31	321	-21	112
T	1.42	0.46	0.82	0.81	0.14	0.46	0.61	0.31	0.39	682	4	325	294	-42	173	389	46	153
M	1.32	0.36	1.01	0.69	0.02	0.97	0.64	0.34	0.40	605	-74	113	250	-87	109	355	12	105
M+	1.30	0.34	1.17	0.85	0.18	1.10	0.45	0.16	0.15	633	-46	93	306	-30	34	327	-15	95

5

1 Table 5. Spatial correlations between simulated average annual CH₄ emissions and GIEMS
 2 surface water area fraction (F_w).

Model	Correlation	Model	Correlation	Model	Correlation
CLM4Me	0.69	LPJ-WHyMe	0.45	UW-VIC (GIEMS)	0.44
DLEM	0.70	LPJ-WSL	0.97	UW-VIC (SWAMPS)	0.11
DLEM2	0.21	LPX-BERN (N)	0.41	VIC-TEM-TOPMODEL	0.41
IAP-RAS	-0.03	LPX-BERN (DYPTOP-N)	0.28	VISIT (GLWD)	0.62
LPJ-Bern	0.56	ORCHIDEE	0.61	VISIT (Sheng)	0.65
LPJ-MPI	0.01	SDGVM	0.09		

3

4 Table 6. Mean CH₄ emissions from LPX-BERN, 1993-2010, for the entire WSL and the
 5 South and North halves of the domain.

Configuration	Mean [TgCH ₄ y ⁻¹]		
	WSL	South	North
LPX-BERN	3.81	1.98	1.83
LPX-BERN (DYPTOP)	3.17	1.38	1.79
LPX-BERN (N)	3.08	1.92	1.17
LPX-BERN (DYPTOP-N)	2.44	1.37	1.08
Differences			
LPX-BERN (N) – LPX-BERN	-0.73	-0.06	-0.66
LPX-BERN (DYPTOP-N)			
– LPX_BERN (DYPTOP)	-0.73	-0.02	-0.71
LPX-BERN (DYPTOP)			
– LPX-BERN	-0.64	-0.60	-0.04
LPX-BERN (DYPTOP-N)			
– LPX-BERN (N)	-0.64	-0.55	-0.09

6

7 Table 7. Temporal Coefficients of Variation (CV) of annual CH₄ emissions, 1993-2004

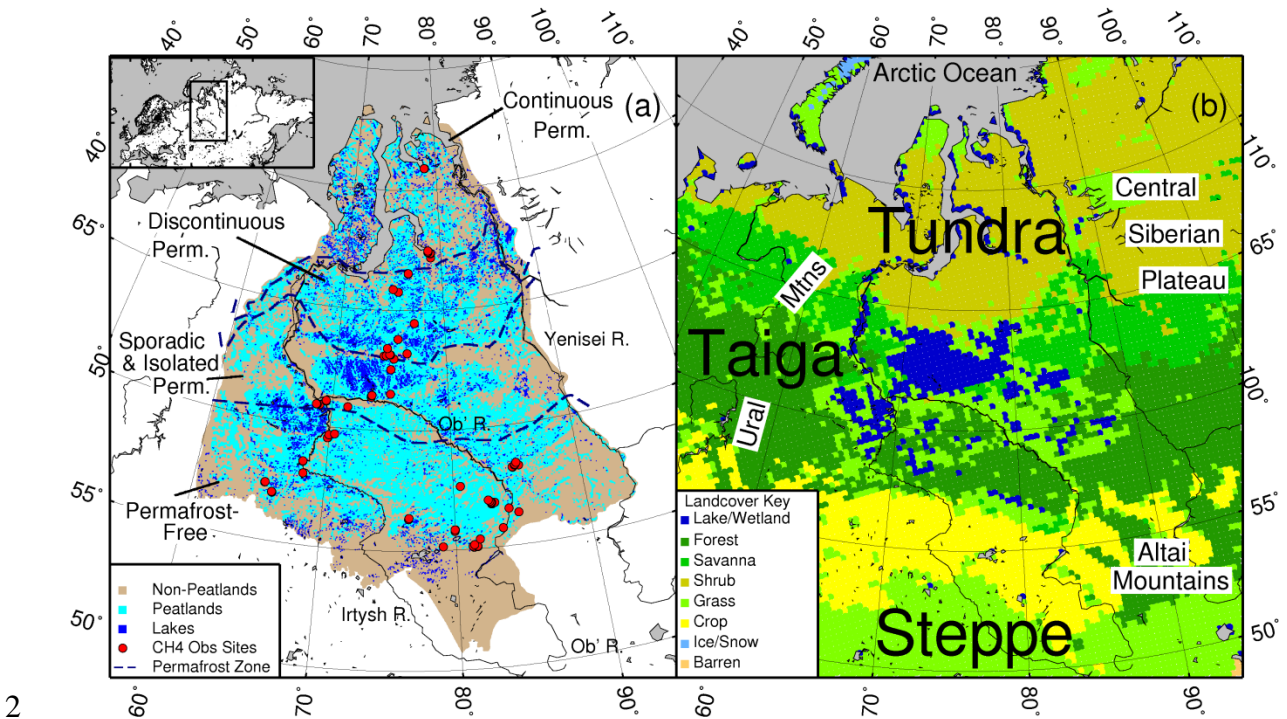
Model	CV	Model	CV	Model	CV
CLM4Me	0.115	LPJ-WSL	0.208	VIC-TEM-TOPMODEL	0.149
DLEM	0.242	LPX-BERN (N)	0.069	VISIT (GLWD)	0.171
DLEM2	0.140	LPX-BERN (DYPTOP-N)	0.076	VISIT (Sheng)	0.163
IAP-RAS	0.091	ORCHIDEE	0.113	Bousquet2011K	0.160
LPJ-Bern	0.087	SDGVM	0.118	Bousquet2011R	0.446
LPJ-MPI	0.195	UW-VIC (GIEMS)	0.338		
LPJ-WHyMe	0.127	UW-VIC (SWAMPS)	0.197		

1

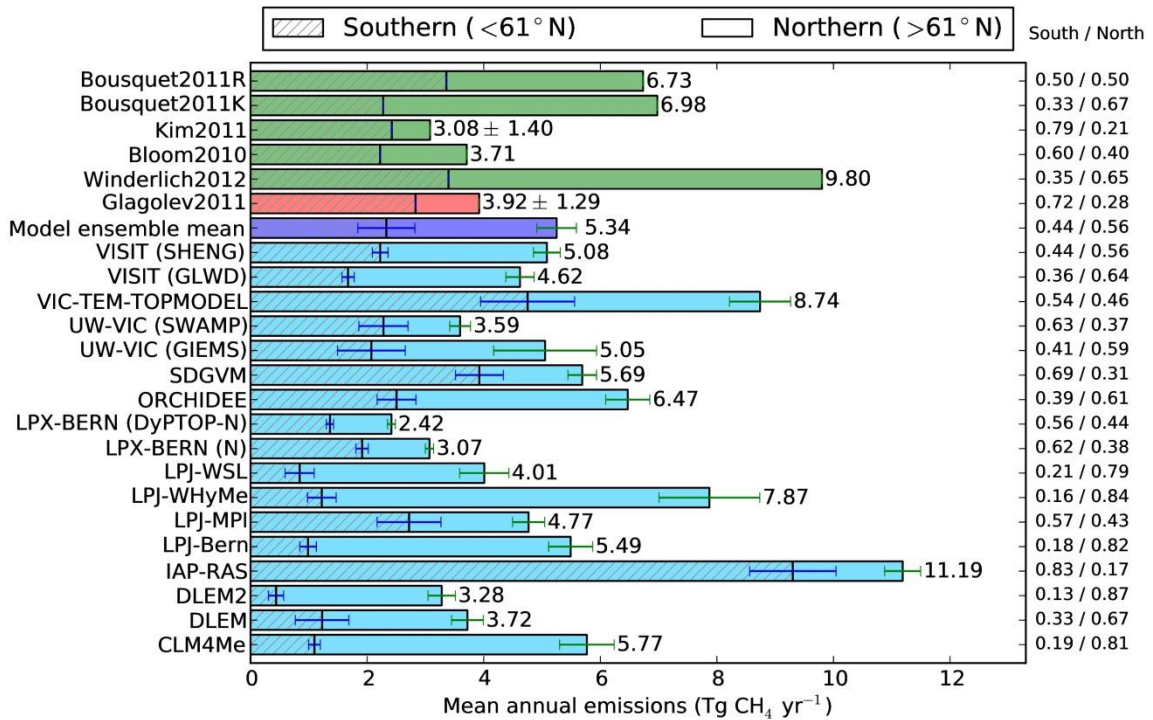
2 Table 8. Temporal correlations among environmental drivers, 1993-2004

WSL	CRU T JJA	CRU P JJA	SWAMPS JJA	GIEMS JJA
CRU T JJA	1.00			
CRU P JJA	-0.10	1.00		
SWAMPS JJA	0.14	0.66	1.00	
GIEMS JJA	-0.11	0.44	0.68	1.00
S	CRU T JJA	CRU P JJA	SWAMPS JJA	GIEMS JJA
CRU T JJA	1.00			
CRU P JJA	-0.28	1.00		
SWAMPS JJA	-0.12	0.44	1.00	
GIEMS JJA	-0.10	0.22	0.87	1.00
N	CRU T JJA	CRU P JJA	SWAMPS JJA	GIEMS JJA
CRU T JJA	1.00			
CRU P JJA	-0.06	1.00		
SWAMPS JJA	0.32	0.60	1.00	
GIEMS JJA	-0.05	0.34	0.61	1.00

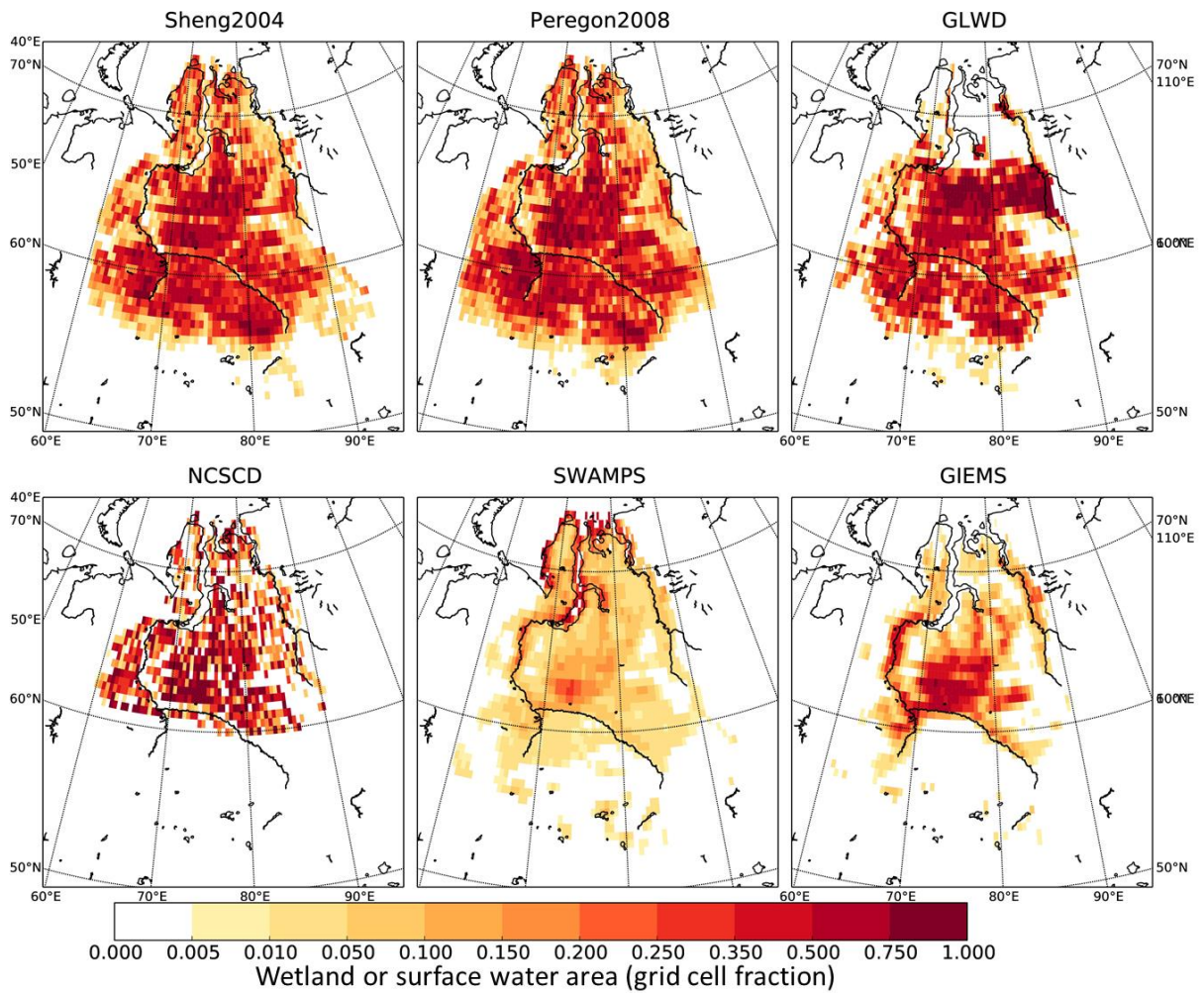
1 Figures



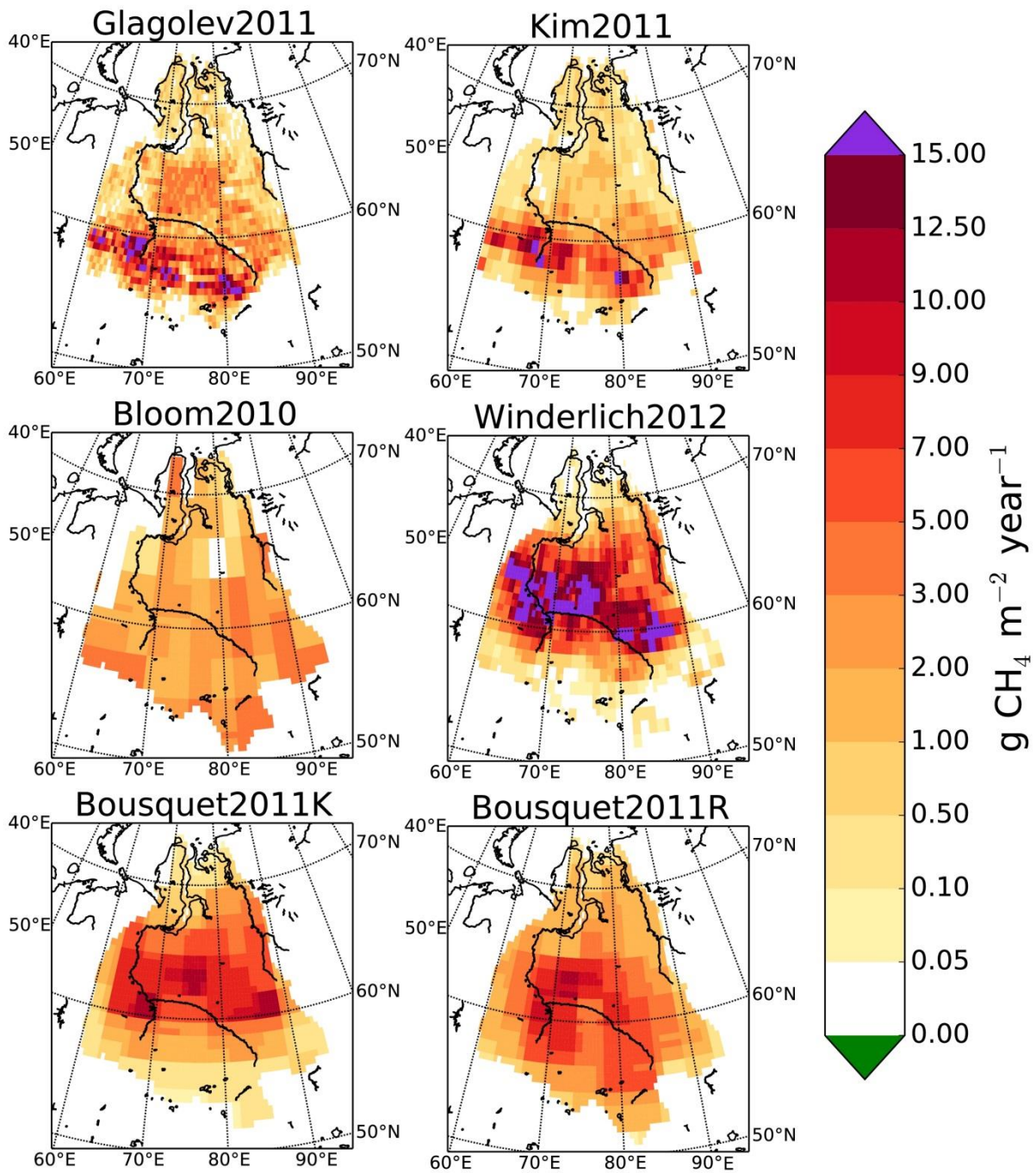
2
3 Figure 1. Map of the West Siberian Lowland (WSL). Panel (a) Limits of domain (brown) and
4 peatland distribution (cyan), taken from Sheng et al. (2004); lakes of area $> 1\text{km}^2$ taken
5 from Lehner and Döll (2004); permafrost zone boundaries after Kremenetski et al. (2003);
6 CH₄ sampling sites from Glagolev et al. (2011) denoted with red circles. Panel (b) Dominant
7 land cover at 25km derived from MODIS-MOD12Q1 500m land cover classification (Friedl
8 et al., 2010).



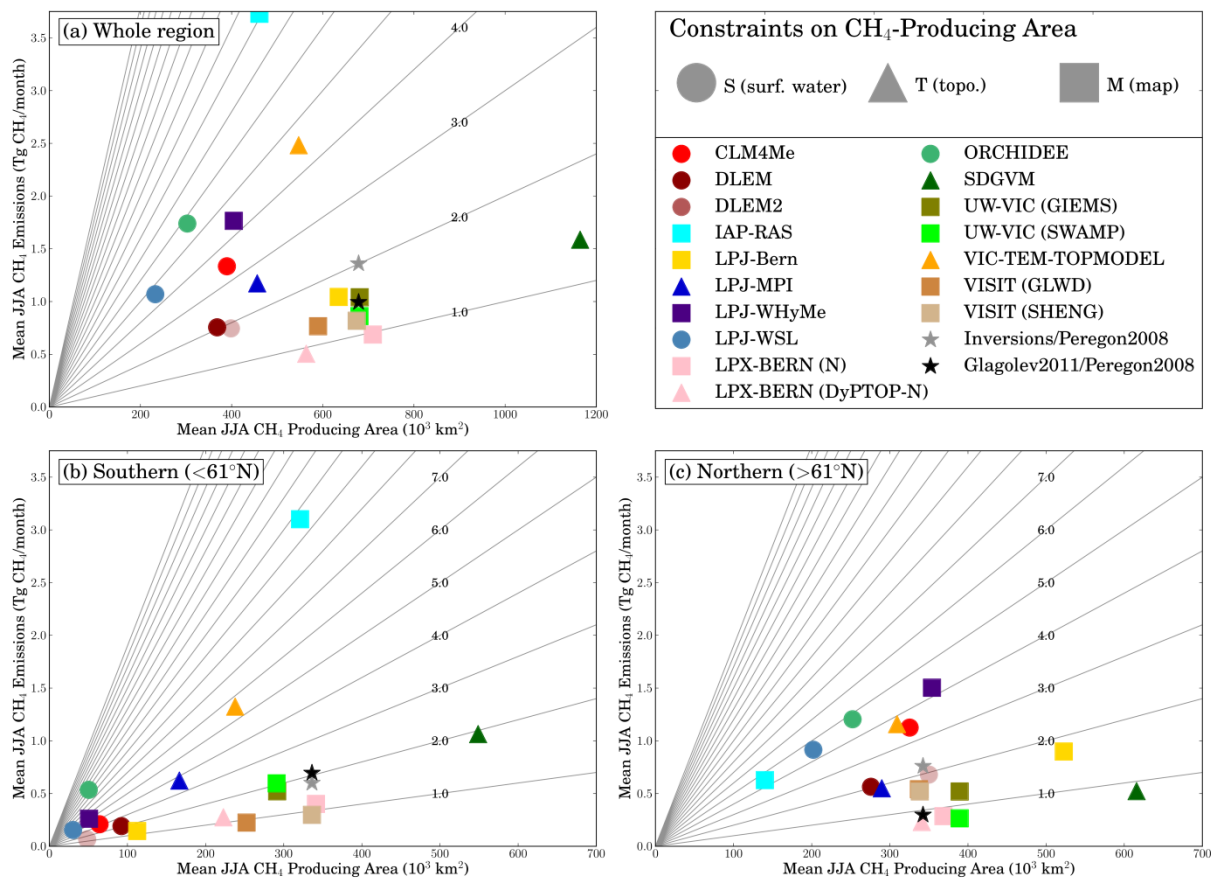
1
 2 Figure 2. Mean annual emissions from the WSL, from inversions (green), observation-based
 3 estimates (red), and forward models (blue). The hatched portions of the bars indicate the
 4 emissions from the southern half of the domain (latitude < 61° N). Error bars on the model
 5 results indicate the interannual standard deviations of the southern and northern emissions.
 6 Error bars on the inversions and observational estimates indicate the uncertainty given in
 7 those studies. Numeric fractions of the total emissions contributed by the southern and
 8 northern halves of the domain are displayed in the right-hand column.



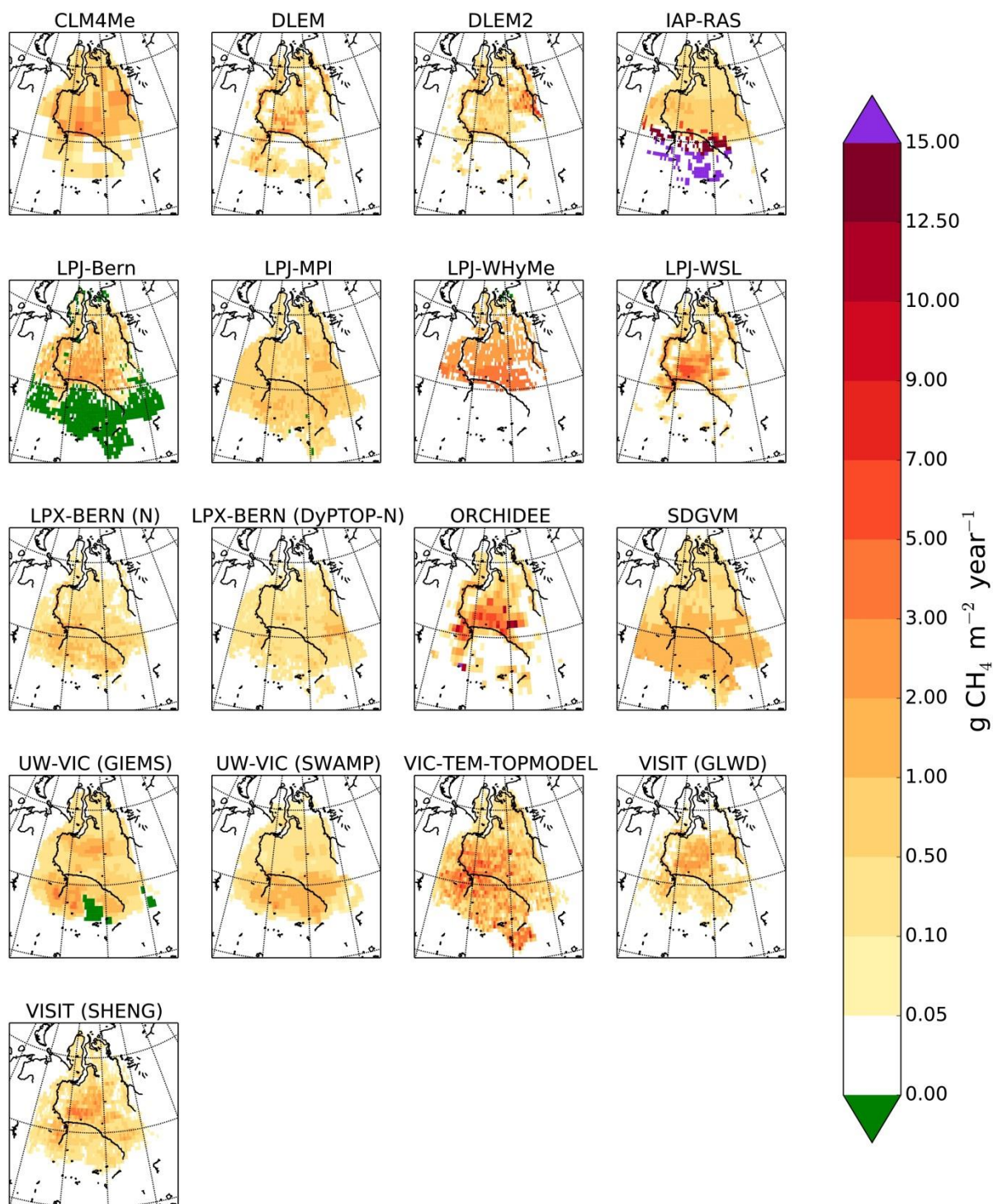
1
 2 Figure 3. Observational datasets related to wetland areas. For SWAMPS and GIEMS, areas
 3 shown are the June-July-August (JJA) average surface water area fraction over the period
 4 1993-2004.



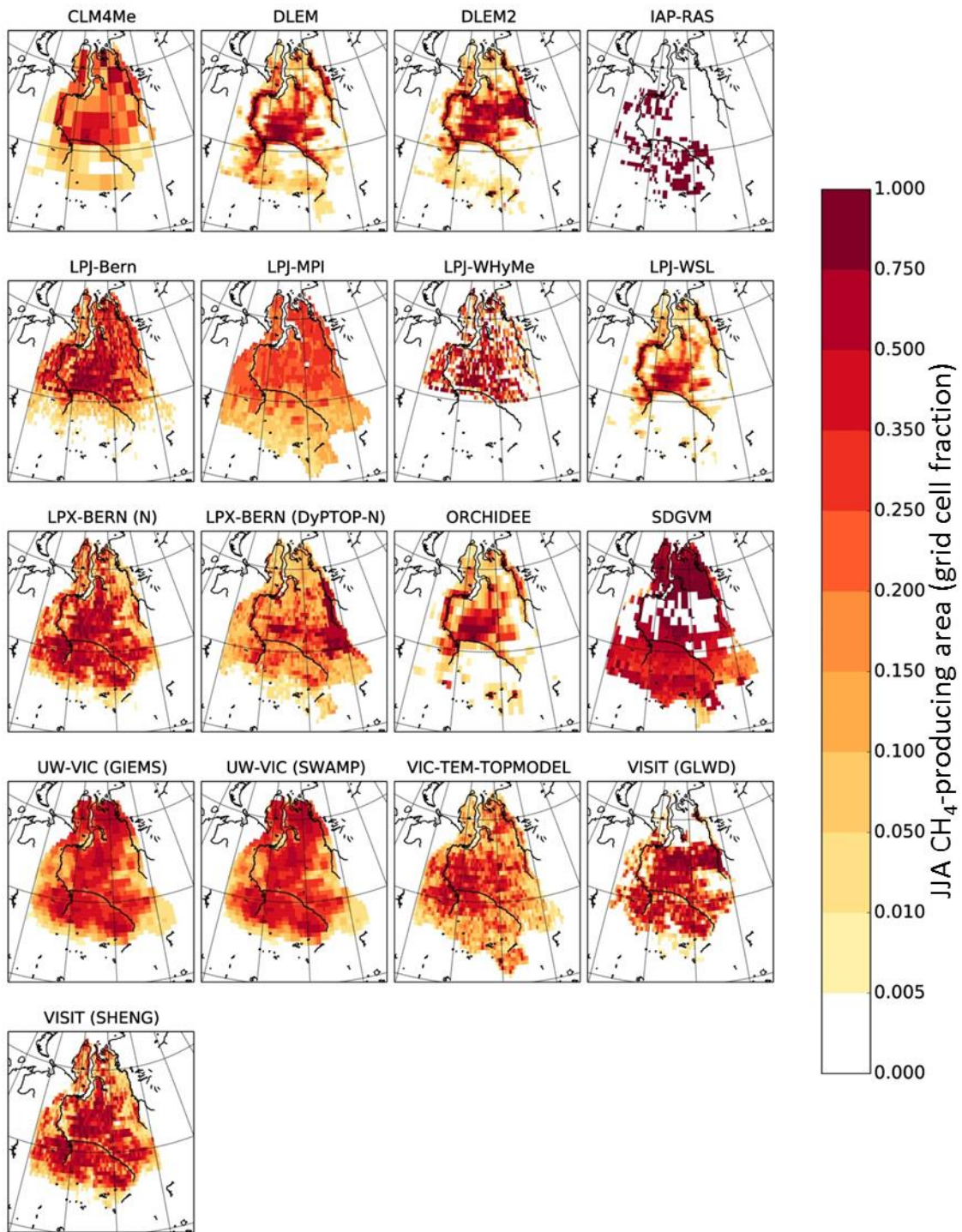
1
 2 Figure 4. Observation- and inversion-based estimates of annual CH₄ emissions (g CH₄ y⁻¹ per
 3 m² of grid cell area). For inversions, averages are over the following periods: 2002-2007
 4 (Kim2011), 2003-2007 (Bloom2010), 2009 (Winderlich2012), and 1993-2004
 5 (Bousquet2011K and R).



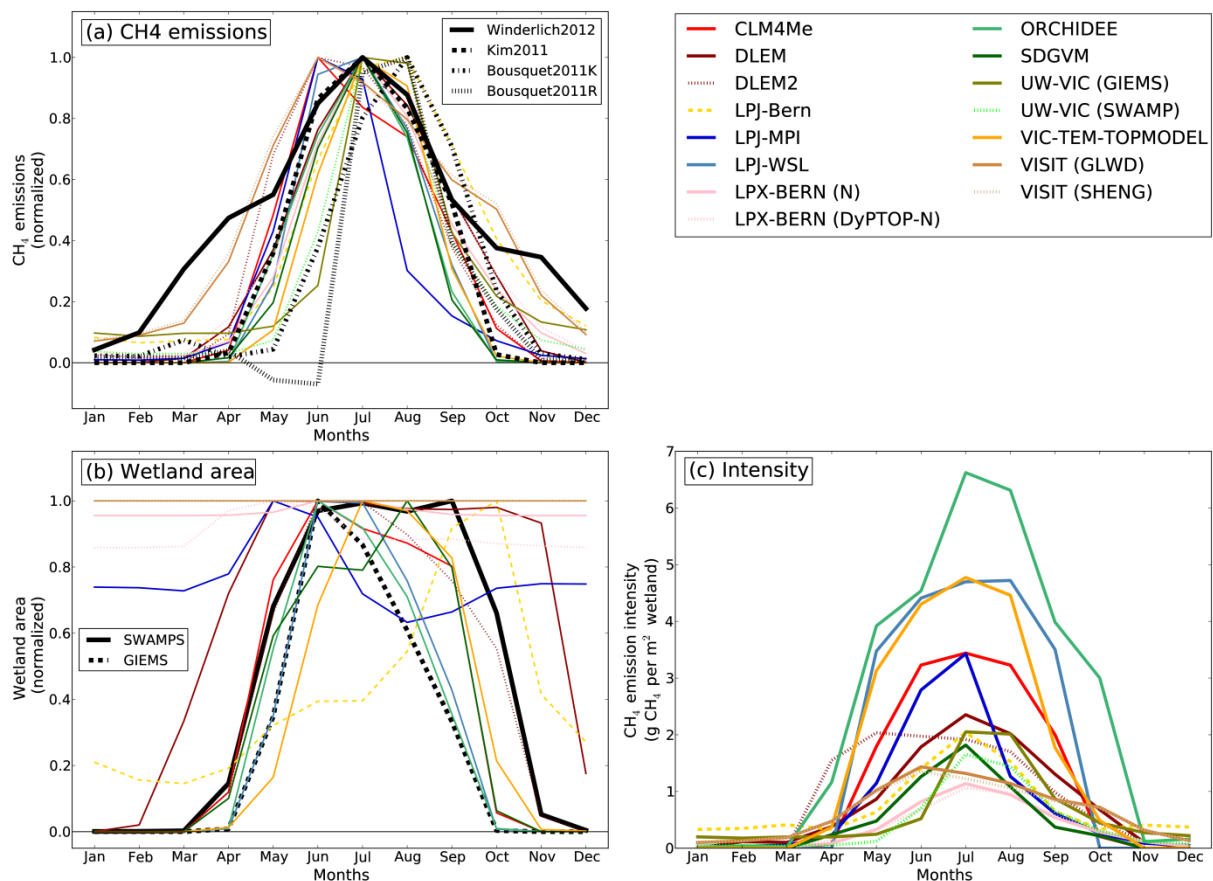
1
 2 Figure 5. Model estimates of JJA CH₄ emissions (Tg CH₄ mon⁻¹) and JJA wetland or CH₄-
 3 producing area (10³ km²), for the entire WSL (top left) and the Southern (bottom left) and
 4 Northern (bottom right) halves, for the period 1993-2004. Lines passing through the origin,
 5 with slopes of integer multiples of 1 g CH₄ m⁻² mon⁻¹, allow comparison of spatial average
 6 intensities (CH₄ emissions per unit CH₄-producing area). Circles denote models that used
 7 satellite surface water products alone (corresponding to code “S” in Table 2) to delineate
 8 wetlands. Triangles denote models that used topographic information, with or without surface
 9 water products (corresponding to code “T” in Table 2). Squares denote models that used
 10 wetland maps with or without topography or surface water products (corresponding to code
 11 “M” in Table 2).



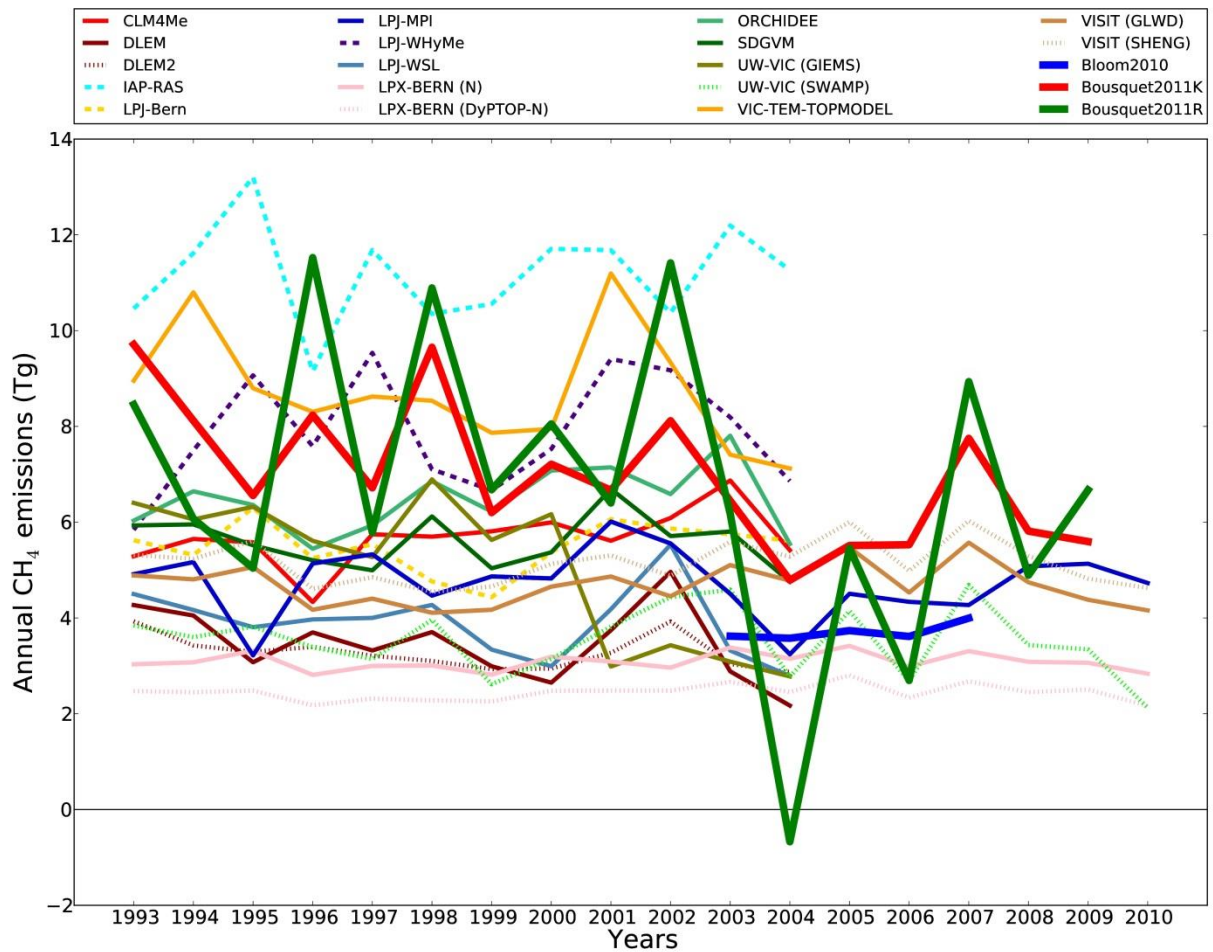
1
2 Figure 6. Maps of simulated average annual CH₄ emissions (g CH₄ m⁻² y⁻¹ of grid cell area).



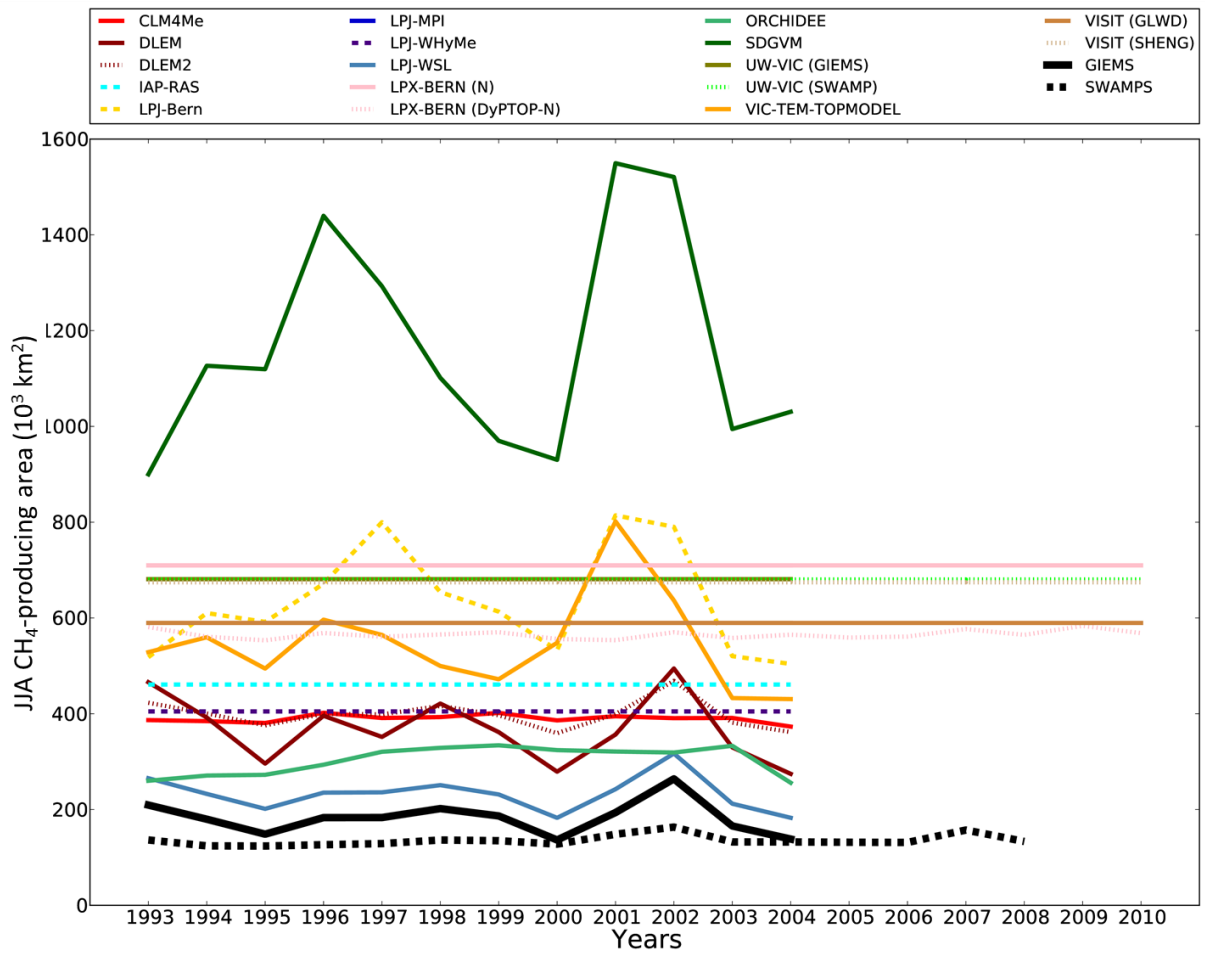
1
 2 Figure 7. Maps of average JJA CH₄-producing area (fraction of grid cell area) from
 3 participating models.



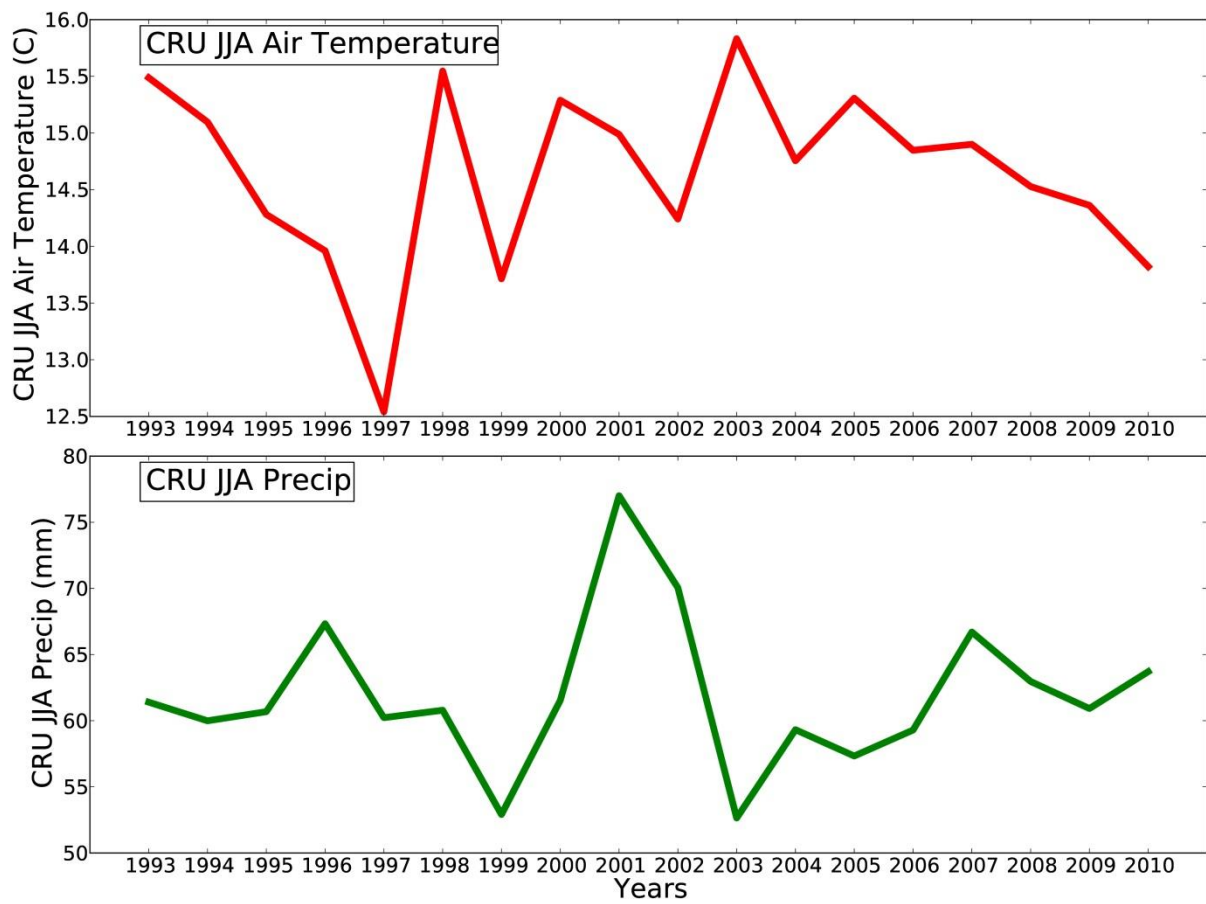
1
 2 Figure 8. Average whole-domain seasonal cycles (1993-2004) of normalized monthly CH₄
 3 emissions (top), normalized monthly CH₄-producing or surface water areas (lower left), and
 4 monthly intensities (g CH₄ per m² of wetland area; lower right), with satellite surface water
 5 products and inversions for reference. CH₄ emissions and areas have been normalized
 6 relative to their peak values.



1
 2 Figure 9. Timeseries of simulated annual total CH₄ emissions (Tg CH₄) from participating
 3 models, the Reference and Kaplan inversions from Bousquet et al. (2011), and the Bloom
 4 (2010) inversion.

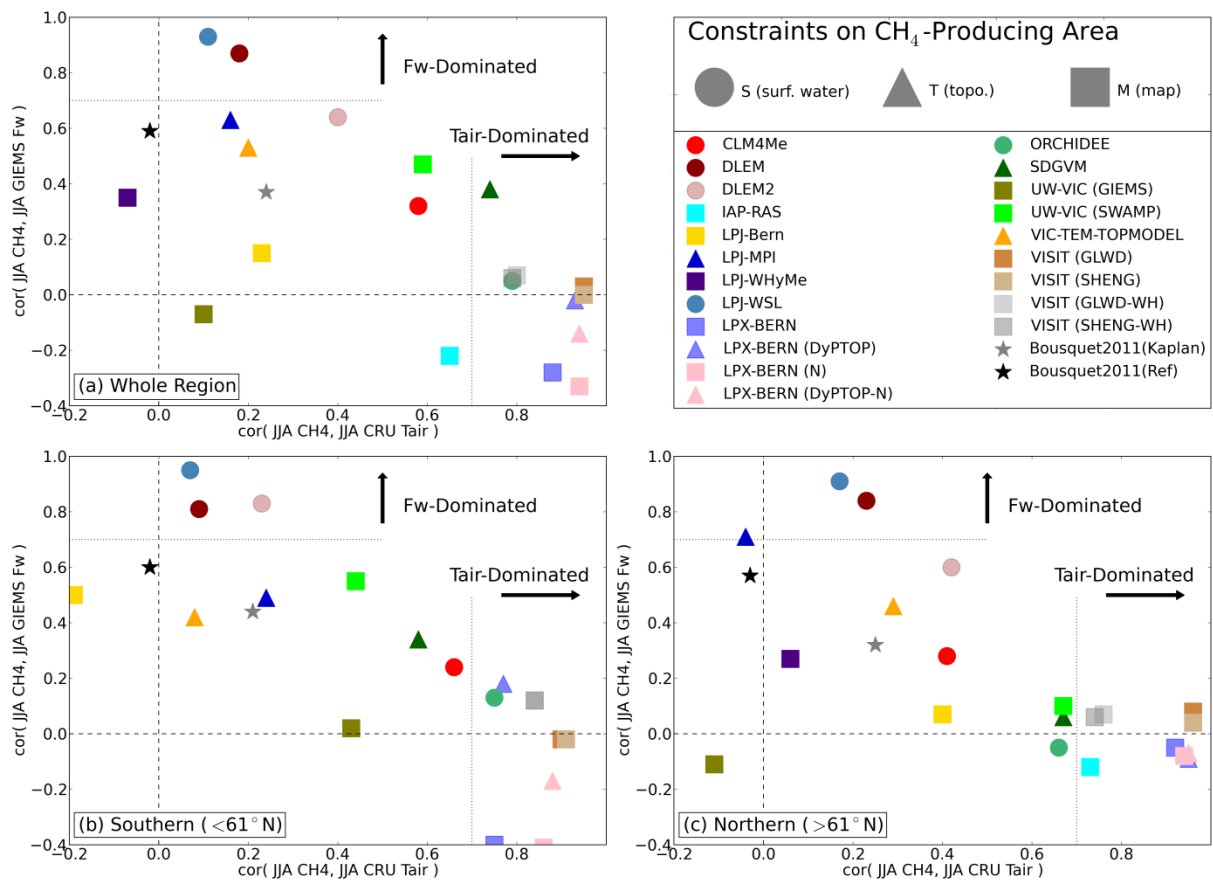


1
 2 Figure 10. Timeseries of simulated JJA CH₄-producing areas (10³ km²), with JJA surface
 3 water areas from GIEMS and SWAMPS products for reference.



1
2

Figure 11. Timeseries of CRU JJA air temperature (°C) and precipitation (mm).



1
2 Figure 12. Influence of interannual variations in surface water area fraction (F_w) on model
3 CH_4 emissions (expressed as correlation between JJA GIEMS F_w and JJA CH_4) vs influence
4 of air temperature (T_{air}) on model CH_4 emissions (expressed as correlation between JJA CRU
5 T_{air} and JJA CH_4), for the entire WSL (top) and the Southern and Northern halves of the
6 domain (bottom). “F_w-Dominated” and “T_{air}-Dominated” denote correlation thresholds above
7 which surface water area or air temperature, respectively, explain more than 50% of the
8 variance of CH_4 emissions. Circles denote models that used satellite surface water products
9 alone (corresponding to code “S” in Table 2) to delineate wetlands. Triangles denote models
10 that used topographic information, with or without surface water products (corresponding to
11 code “T” in Table 2). Squares denote models that used wetland maps with or without
12 topography or surface water products (corresponding to code “M” in Table 2).